A Novel Technique Of Power Flow Controller By Using A DC Current Flow Controller For Meshed Modular Multilevel Converter Three-Terminal HVDC Grids

A Thesis Submitted In Partial Fulfilment Of

the Requirements for the Award of the Degree Of

MASTER OF TECHNOLOGY

In

ELECTRICAL ENGINEERING

With Specialization

In

POWER SYSTEM ENGINEERING

By

MAYTHAM KHUDHAIR ABBAS

Y15MTPS927

Under the esteemed guidance of

Dr.Ch. Ravi Kumar

M.Tech , Ph.D. Asst. Prof.

DEPARTMENT OF ELECTRICAL & ELECTRONIC ENGINEERING

UNIVERSITY COLLEGE OF ENGINEERING & TECHNOLOGY

ACHARYA NAGARJUNA UNIVERSITY

NAGARJUNA NAGAR ,GUNTUR – 522510- A.P

2016-2017

DEPARTMENT OF ELECTRICAL & ELECTRONIC ENGINEERING
UNIVERSITY COLLEGE OF ENGINEERING & TECHNOLOGY
ACHARYA NAGARJUNA UNIVERSITY
NAGARJUNA NAGAR ,GUNTUR – 522510- A.P

CERTIFICATE

This is to certify that it is a bonafied work on **"A Novel Technique Of Power Flow Controller By Using A DC Current Flow Controller For Meshed Modular Multilevel Converter Three-Terminal HVDC Grids "** has been submitted by **Mr MAYTHAM KHUDHAIR ABBAS (Y15MTPS927)** in partial fulfillment of the requirement of the award of the degree of **Master of Technology** in Electrical Engineering with specialization in **POWER SYSTEM ENGINEERING** At Acharya Nagarjuna University, Guntur, during the academic year 1st sept 2015 to 31st Aug 2017. The candidate worked right under my supervision and guidance.

PROJECT GUIDE
Dr.Ch. Ravi Kumar, M.Tech, Ph.D
Assist. Prof, Dept. of EEE

HEAD OF THE DEPT.
Dr. P.V. Ramana Rao M.Tech., Ph. D
Prof. and HOD, Dept. EEE

DEAN OF ANU CET
Prof. P. Siddaiah
Professor

DIRECTOR OF ANU I.S.C
Prof . G.V.S.R Anjaneyulu
Professor

ACKNOWLEDGEMENT

It gives me immense pleasure to take this opportunity to express my sincere and heartfelt thanks to ***Dr.CH. RAVI KUMAR M.Tech.,Ph.D Asst.Prof*, *Dept.*** of Electrical & Electronic Engineering, Acharya Nagarjuna University College of Engineering and Technology, Guntur, for his able and continual guidance and help throughout the entire period of investigation.

I express my sincere thanks to the authorities of Acharya Nagarjuna University, Dean ***Prof. P.SIDDAIAH*** A.N.U College of Engineering and ***Dr.P.V.Ramana Rao M.Tech.,Ph.D*** Head, Department of Electrical & Electronic Engineering, for the help in extending the laboratory facility to carry out the experiments and permitting me to complete me to complete the work.

I am grateful to the faculty of Dept. Electrical & Electronic Engineering, for their moral support and encouraging words during the course of work..

I am very much thankful to ***Prof . G.V.S.R Anjaneyulu***, Director of International student cell.

MAYTHAM KHUDHAIR ABBAS

(Reg. no.) Y15MTPS927

DEDICATION

TO MY BELOVED WHO GOD MAKES THE PARADISE UNDER HER FEET,

TO THE KINDNESS WHICH GIVES ME THE CONSTANCY,

TO MY DEAR MOTHER,

TO WHO LIGHTS MY PATH AND GIVES ME HIGH MORALS,

TO THE SEA WHO PULSATES GIVING,

MY DEAR FATHER,

TO THE ADDRESS OF IMAGES OF MY CHILDHOOD,

TO WHO I LIVE OF THEM,

MY BROTHERS AND SISTERS.

ABSTRACT

This thesis proposes the design of a novel DC current flow controller (CFC) and evaluates the control performance of balancing and regulating the DC branch currents using the DC CFC in a meshed multi-terminal HVDC (MTDC) grid.

The DC CFC consists of two identical full bridge DC-DC converters with the capacitors of the two converters being connected in parallel. The scalability of the DC CFC is easily achievable due to the identical bridge converter topology; the cost of this DC CFC is also relatively low due to its simple physical structure and low voltage ratings.

The control performance of the DC CFC is tested on a meshed 3-terminal (3-T) HVDC grid, which is based on modular multilevel converters (MMC). The DC branch current control in the meshed MTDC grid is achieved using the proposed control strategy of the DC CFC, and is verified through case studies on the real-time digital simulator (RTDS).

List Of Symbols

LCC	Line Commutated Converters
VSC	Voltage Source Converters
μ	Overlap angle
M	Ratio of the ideal converter
$\mathbf{V_{VSC}}$	VSC terminal voltage
$\mathbf{V_{line}}$	DC line voltage
$\boldsymbol{T}$	Terminal station
$\boldsymbol{L_{12}}$	The link 1-2
$\boldsymbol{I_{L12}}$	Current in line 1-2
$\mathbf{I_{SR}}$	Current source in primary side of Transformer
$\mathbf{C_E}$	A capacitor in primary side of Transformer
$\mathbf{U_{SR}}$	Voltage source in secondary side of Transformer
$\boldsymbol{I_{dref}}$	Expected current of DC line
$\boldsymbol{I_d}$	Actual current
$\mathbf{U_0}$	Rated voltage of the DC grid
K	Ratio of the voltage between the primary and secondary side
$\boldsymbol{V_{PFCref}}$	generates a reference voltage
D1, D4 and D6	Diodes
S2, S3 and S5	Switches
$\mathbf{I_{12}, I_{13}, I_{23}}$	lines current
$\boldsymbol{D_{s2A}, D_{s2B}}$	The duty cycle of switch S2 for pair A and B
$\mathbf{\bar{I}_{cA}, \bar{I}_{cB}}$	The average current through the capacitor

ΔE_{ripple}	The voltage ripple
f	The switching frequency
|E|	The real average voltage of capacitor
$\mathbf{I_1, I_2, I_3}$	DC terminal currents
$\mathbf{I_{12}, I_{23}, I_{13}}$	DC branch currents
V_1, V_2, V_3	DC terminal voltages
V_C	The voltage of the interconnected capacitor
$\Delta P_1, \Delta P_2$	Power exchange of the interconnected capacitors
G_A	controlled gating signal
I_{12meas}	The measurement of branch current 12
I_{12ref}	The reference of branch current 12
$\mathbf{P_c}$	The power of the capacitor
N_P, N_N	The interconnection points are the positive and negative side of the capacitor
S_1, S_2	two switching valves
V_{SM}	The output voltage of each SM
L_{arm}	series inductor per converter arm
n-T	n-terminal
T_n	Terminal-n

CONTENT

Chapter Two: Power Flow Controller for The Meshed DC Grids

Chapter Three: A DC CFC for Meshed Modular Multilevel Converter Multi-terminal HVDC Grids

Chapter-I

Introduction

CHAPTER ONE

INTRODUCTION

HVDC System

This chapter presents general aspects of high-voltage direct current (HVDC) transmission. Firstly, a comparison between HVDC and high-voltage alternating current (HVAC) transmission systems is presented. Two major HVDC technologies, i.e., LCC based and VSC based HVDC transmission are described in addition to the different HVDC configurations.

The chapter also discusses general overview on Multi-terminal HVDC system and need of DC/DC converters in MTDC system.

1.1 Introduction

The history of transmission of electricity started way back in 1882, when a 57 km long, 1.4kV DC transmission line from Miesbach to Munich was constructed [1].

The DC system developed during this period was operating with the same voltage from generation till consumption due to the lack of a device which could transform the DC voltage.

This resulted in using very costly huge conductors even for distribution, thus forcing to build generating stations near to the load centres. With the development of AC transformer during the late 1880, transmission through DC lost interest as AC power now could be transmitted over long distances at a high voltage, thereby reducing the transmission losses and then can be stepped down to a level suitable for the consumer loads.

In spite of the use of AC system for transmission of electric power, there were many focus towards DC transmission in the early 20th century [2].

Ever since the first mercury arc based HVDC system with a capacity of 20MW, operating at 100kV DC was built in 1945, there was a steady increase in HVDC schemes commissioned worldwide.

The recent developments in the power electronics industry has changed the way the transmission is going to be in the future with HVDC system.

1.2 HVDC vs HVAC System

Transmission through HVDC has many distinct advantages over HVAC scheme . Some of them are listed below.

- For the similar insulation level and cross sectional area, DC lines can carry $\sqrt{2}$ times more power than AC.
- Right of way requirement for carrying electric power using DC lines are smaller than AC for the same power. In other way, for the same right of way, more power can be transmitted using DC system.
- The DC transmission losses are less as compared to AC, thereby providing increased efficiency.
- AC system possess both skin and proximity effect. It restricts maximum utilization of conductors for the transmission, which is completely absent in the DC system.
- Easy to implement the active power control in HVDC
- With both active and reactive current component present in the AC power, the useful power transmitted is always limited as shown in the figure 1.1.

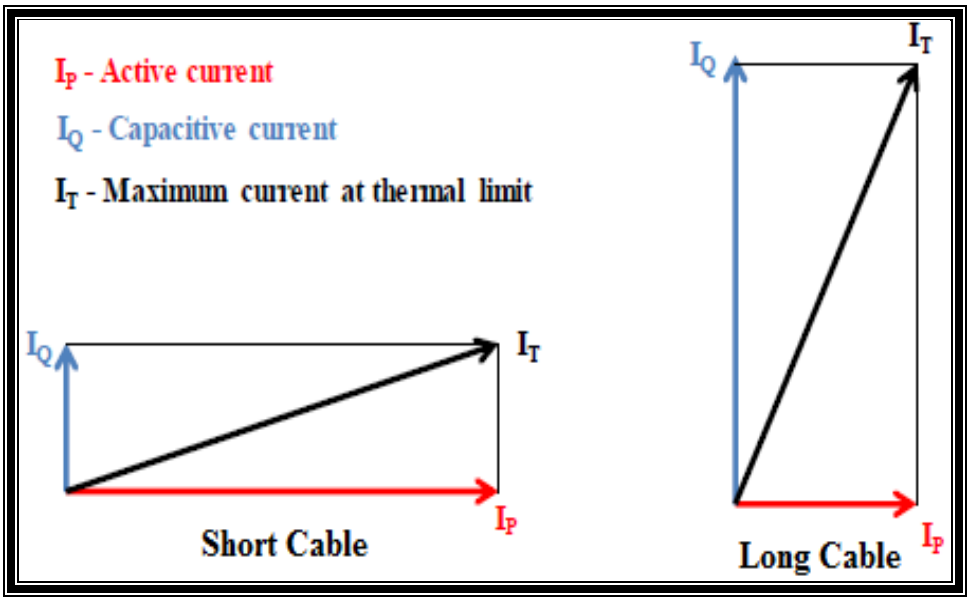

Fig. 1.1 HVAC Cable current limit

This issue is further aggravated when the transmission of power is through AC cables. With increase in the cable length, capacitive nature of cable increases, resulting more charging current in the cable and restricting the active component of current .

In order to overcome this problem, reactive compensation is required, which in-turn increases the cost and space requirement. However, a DC transmission involves no reactive elements and does not require any reactive compensation.

In addition to the above benefits, HVDC scheme also facilitate the interconnection of two asynchronous AC grid operating with different frequencies using back-to-back HVDC configuration. With all the above advantages mentioned above, the cost of converter is always a concern for HVDC system. Considering the cost of converters, other associated equipments and transmission losses, HVDC is economical for the transmission of electrical power when the distance is higher than the breakeven distance of figure 1.2.

The breakeven distance for overhead line is 500-800km, while for submarine cables, it is around 50-60km.

To summarise with, HVDC systems is the preferred option for carrying bulk power over a very long distance, interconnection of asynchronous grids, power transmission through submarine cable etc.

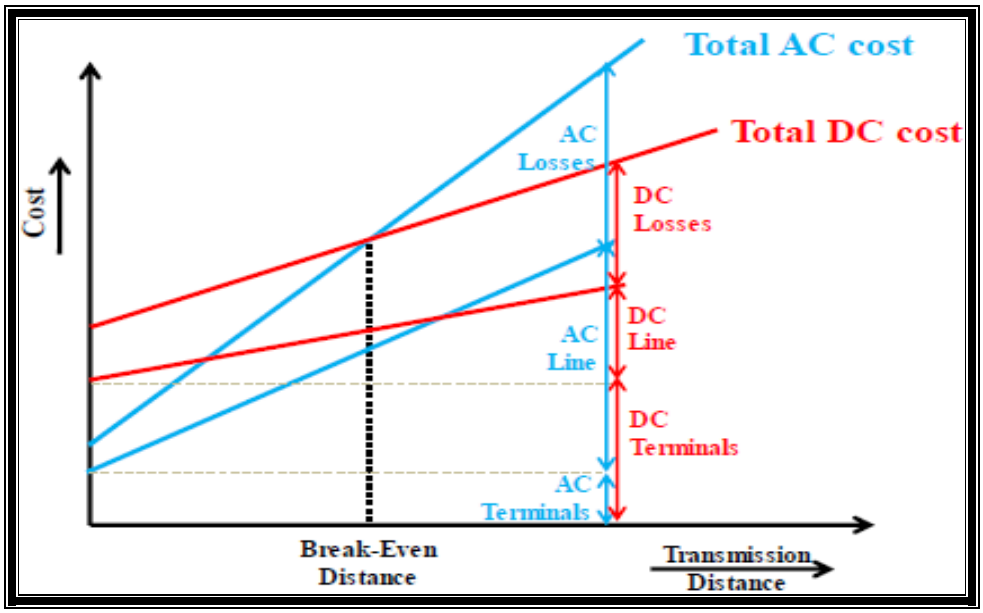

Fig. 1.2 Cost comparison of AC/DC

1.3 Converter Technology

HVDC transmission in the early days used converter technology based on mercury arc valves. However, with the problem of ark-back fault, the rectifying property of the converter valve gets damaged and consequently results in many other associated problems [2]. HVDC technology currently being employed can be classified as:

- Line Commutated Converters(LCC).
- Voltage Source Converters(VSC).

1.3.1 LCC based HVDC System

1.3.1.1 Six-pulse bridge

The basic LCC configuration for HVDC uses a three-phase Graetz bridge rectifier or six-pulse bridge as show figure 1.3, containing six electronic switches, each connecting one of the three phases to one of the two DC terminals. A complete switching element is usually referred to as a valve, irrespective of its construction. Normally, two valves in the bridge are conducting at any time: one on the top row and one (from a different phase) on the bottom row. The two conducting valves connect two of the three AC phase voltages, in series, to the DC terminals. Thus, the DC output voltage at any given instant is given by the series combination of two AC phase voltages. For example, if valves V1 and V2 are conducting, the DC output voltage is given by the voltage of phase 1 minus the voltage of phase 3.

Because of the unavoidable (but beneficial) inductance in the AC supply, the transition from one pair of conducting valves to the next does not happen instantly. Rather, there is a short overlap period when two valves on the same row of the bridge are conducting simultaneously. For example, if valves V1 and V2 are initially conducting and then valve V3 is turned on, conduction passes from V1 to V3 but for a short period both of these valves conduct simultaneously. During this period, the DC output voltage is given by the average of the voltages of phases 1 and 2, minus the voltage of phase 3. The overlap angle μ (or u) in an HVDC converter increases with the load current, but is typically around 20° at full load. During the overlap period, the output DC voltage is lower than it would otherwise be and the overlap period produces a visible notch in the DC voltage. An important effect of this is that the mean DC output voltage decreases as the overlap period increases, hence the mean DC voltage falls with increasing DC current.

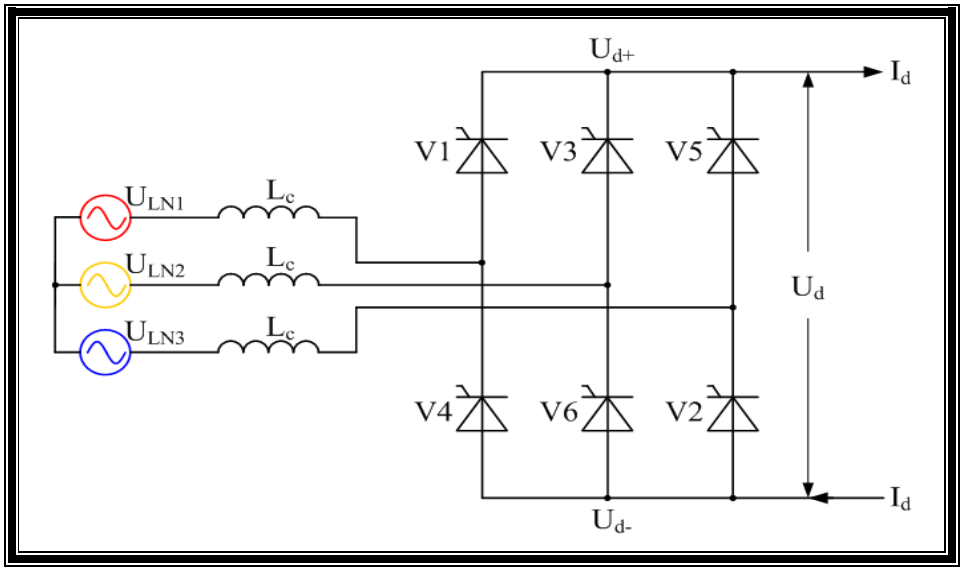

Fig.1.3 Three-phase full-wave (Graetz) bridge rectifier circuit

Commutation process when just valves 1 and 2 are conducting, the DC voltage is formed from two of the three phase voltages. During the overlap period the DC voltage is formed from all three phase voltages as show figure 1.4.

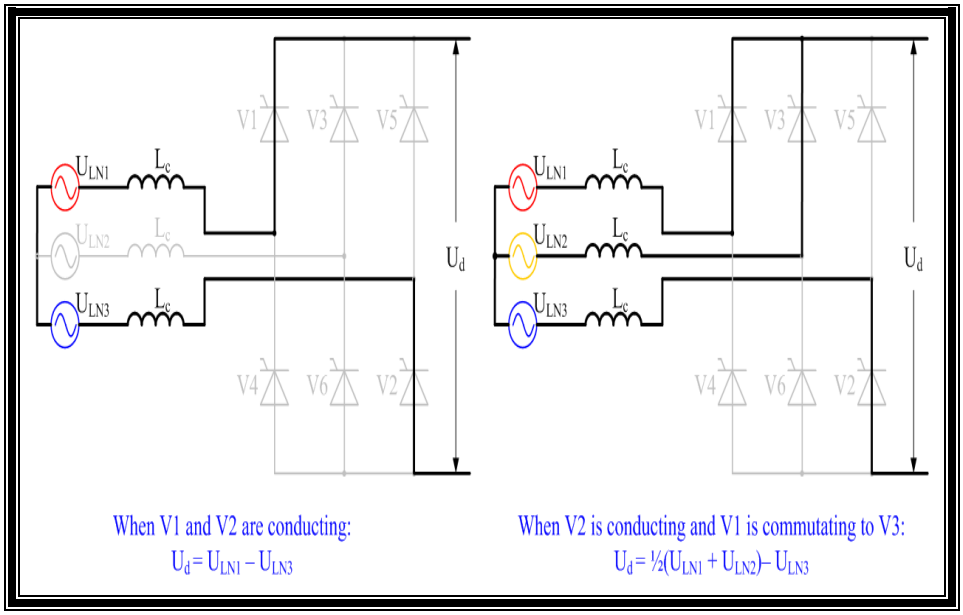

Fig.1.4 Commutation process

1.3.1.2 Twelve-pulse bridge

A 12 pulse LCC based HVDC scheme is shown in the figure 1.5. The system consists of AC filters and capacitor banks, converter transformer, two converter stations for rectification and inversion, DC filters, smoothing reactors(DC reactor) and DC line . The converters use thyristor valves as the power electronic devices for the conversion and are connected in series for the required DC voltage. Thyristors can be only turned **ON** by applying a gate signal, however needs commutation in the form of natural or line commutation to turn **OFF** the device.

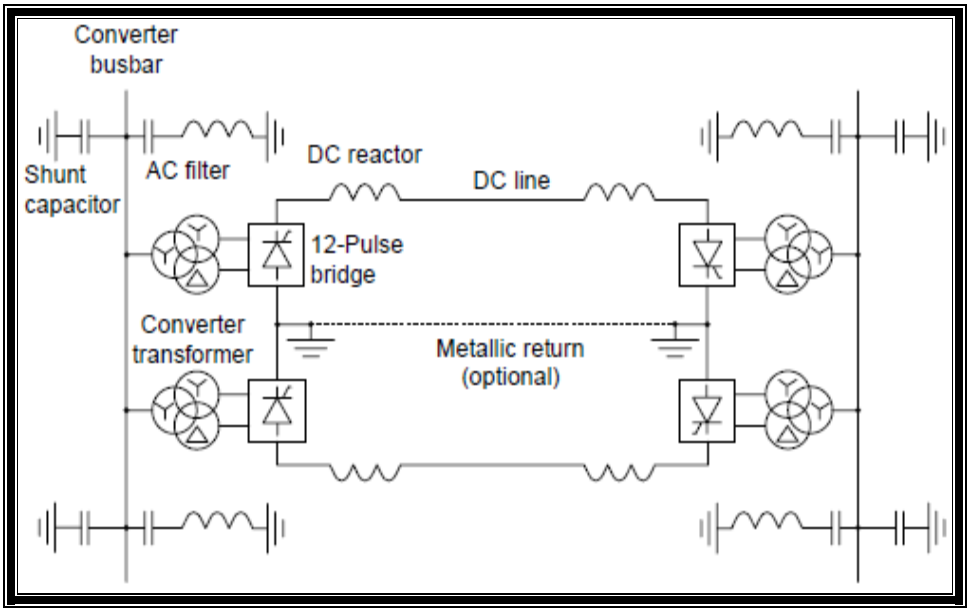

Fig. 1.5 LCC Based HVDC system

Converter transformer provides the necessary AC voltage for the thyristors and also facilitate the 12 pulse operation. AC filters are required to filter out the harmonics present in the AC and DC side. A major drawback of LCC scheme is that it always consumes reactive power in both the rectifier and inverter mode. Depending on the firing angles, the reactive power consumption of an LCC-HVDC converter station is nearly 50-60% of the active power. LCC based HVDC schemes are still the main technology for bulk power transmission over 1000MW. Typical power loss per converter station is only 0.7% of the transmitted active, which is very low. LCC suffers many disadvantages .

- Reactive power requirement for the operation of converters. The reactive power compensation is provided by connecting large capacitor banks at AC side of the converters. This results in increased cost and large amounts of space.
- Failure to commutate current from one valve to the next in sequence. A commutation failure occurs when the incoming valve fails to take over the current before the commutating voltage reverses the polarity, with sufficient extinction time. Although a single commutation failure will not cause any harm to the system, a repeated commutation failures may cause the converter to trip .
- Thyristor based converters require a relatively strong AC voltage source for the commutation purpose. For the successful converter operation, a minimum three-phase symmetrical short circuit capacity equivalent to two times the converter rating is required from the AC network side.

1.3.2 VSC based HVDC System

The latest technology for the HVDC transmission is using Voltage source converters. This was first introduced by ABB in 1990's with the first VSC based HVDC system commissioned at Gotland island of Sweden with a rating of 50MW. The general schematic of VSC based HVDC scheme is shown in the figure 1.6.

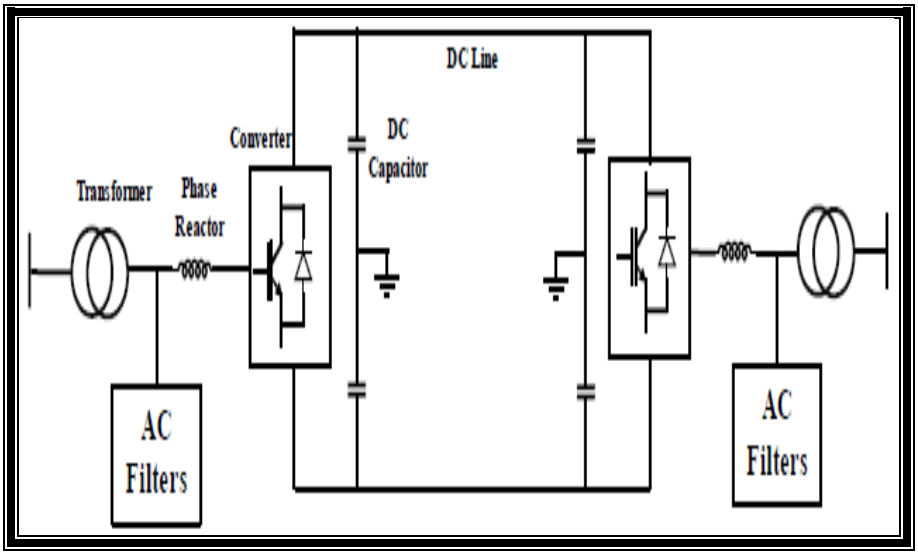

Fig. 1.6 VSC based HVDC system

The system has 2 converters, one at the rectifying side and other at the inverter side. Each converter utilizes self-commutating switches, e.g., GTO or IGBTs, as the power electronic switches for the power conversion.

These devices can be turned **ON** and **OFF** by applying controlled gate pulses. A complete IGBT module consists of an IGBT, an anti-parallel diode, a gate unit, a voltage divider, and a water-cooled heat sink. Each gate unit includes gate-driving circuits, surveillance circuits, and optical interface . The gate driving electronics control the gate voltage and current at turn-on and turn-off to achieve optimal turn-on and turn-off processes of the IGBTs.

An ordinary transformer is connected for providing the voltage level suitable for the converter so as to get the required DC voltage. The phase reactor connected at each phase of the AC side provides low pass filtering for the switching harmonics, active and reactive power control and also limits the short circuit current. Since the gate pulses are provided using PWM technique with high switching frequency, AC filters are provided for eliminating the harmonics in the signal. The DC capacitor provides the stiff DC voltage and a low-inductance path for the turn-off switching currents in addition of serving as an energy storage and reducing the DC voltage harmonics ripples.

1.3.2.1 Two-level converter of VSC-HVDC

From the very first VSC-HVDC scheme installed (the Hellsjön experimental link commissioned in Sweden in 1997) until 2012, most of the VSC HVDC systems built were based on the two level converter. The two-level converter is the simplest type of three-phase voltage-source converter and can be thought of as a six pulse bridge in which the thyristors have been replaced by IGBTs with inverse-parallel diodes, and the DC smoothing reactors have been replaced by DC smoothing capacitors as show figure 1.7. Such converters derive their name from the fact that the voltage at the AC output of each phase is switched between two discrete voltage levels, corresponding to the electrical potentials of the positive and negative DC terminals. When the upper of the two valves in a phase is turned on, the AC output terminal is connected to the positive DC terminal, resulting in an output voltage of $(+\frac{1}{2}U_d)$ with respect to the midpoint potential of the converter. Conversely when the lower valve in a phase is turned on, the AC output terminal is connected to the negative DC terminal, resulting in an output voltage of $(-\frac{1}{2}U_d)$. The two valves corresponding to one phase must never be turned on

simultaneously, as this would result in an uncontrolled discharge of the DC capacitor, risking severe damage to the converter equipment as shown figure 1.8. The simplest (and also, the highest-amplitude) waveform that can be produced by a two-level converter is a square wave; however this would produce unacceptable levels of harmonic distortion, so some form of Pulse-width modulation (PWM) is always used to improve the harmonic distortion of the converter.

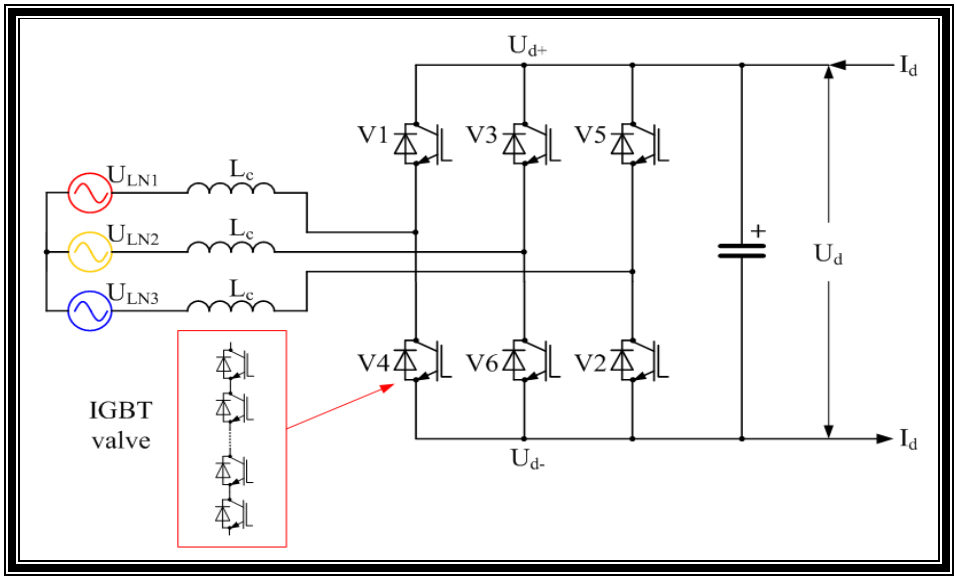

Fig.1.7 VSC base HVDC Two Level

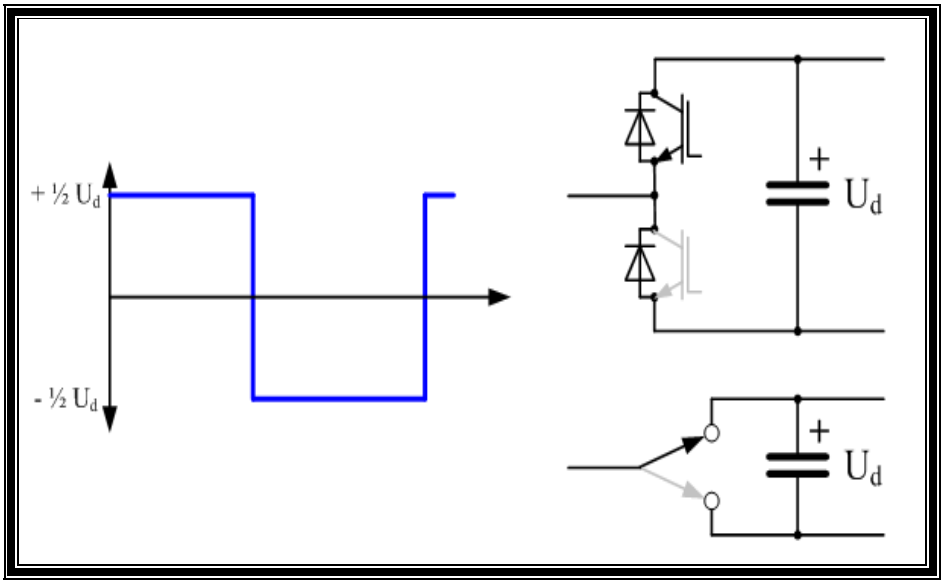

Fig.1.8 Operating principle of 2-level converter, single-phase representation

1.3.2.2 Three-level converter of VSC-HVDC

In an attempt to improve on the poor harmonic performance of the two-level converter, some HVDC systems have been built with three level converters as shown figure 1.9. Three-level converters can synthesize three (instead of only two) discrete voltage levels at the AC terminal of each phase $(+\frac{1}{2}U_d)$,(0) and $(-\frac{1}{2}U_d)$. A common type of three-level converter is the diode-clamped (or neutral-point-clamped) converter, where each phase contains four IGBT valves, each rated at half of the DC line to line voltage, along with two clamping diode valves. The DC capacitor is split into two series-connected branches, with the clamping diode valves connected between the capacitor midpoint and the one-quarter and three-quarter points on each phase.

To obtain a positive output voltage $(+\frac{1}{2}U_d)$ the top two IGBT valves are turned on, to obtain a negative output voltage $(-\frac{1}{2}U_d)$ the bottom two IGBT valves are turned on and to obtain zero output voltage the middle two IGBT valves are turned on. In this latter state, the two clamping diode valves complete the current path through the phase as shown figure 1.10.

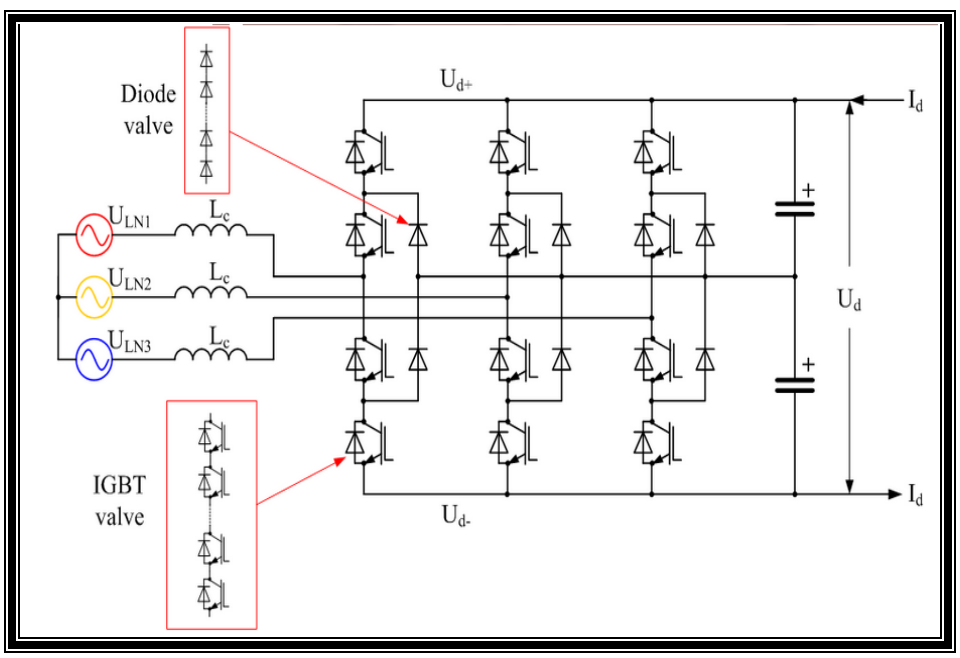

Fig.1.9 Three-phase, three-level, diode-clamped voltage-source converter for HVDC

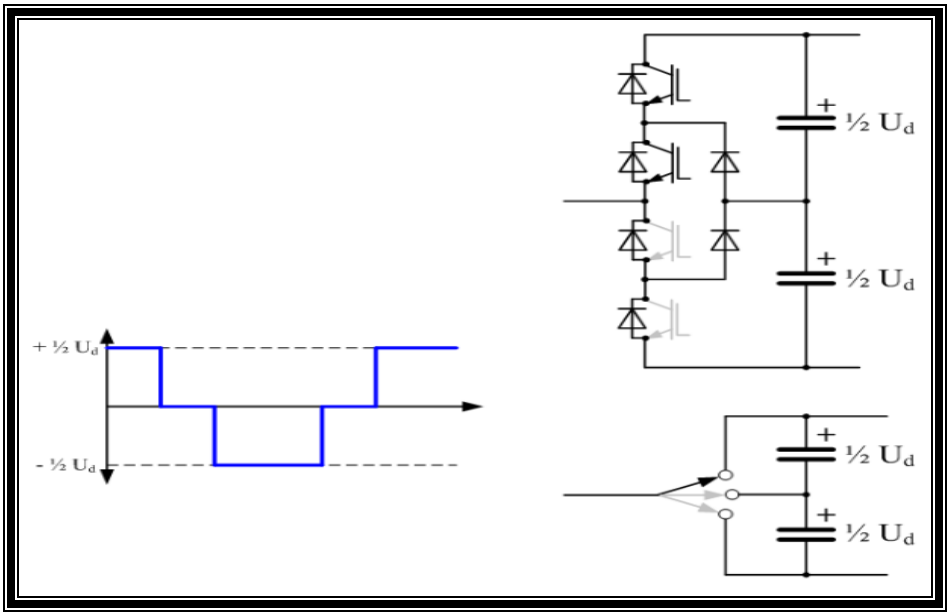

Fig.1.10 Operating principle of 3-level, diode-clamped converter, single-phase representation

VSC based HVDC schemes offer many benefits over conventional LCC based, some of which are listed below.

- Control of both active and reactive power in one equipment. By decoupling active and reactive component of the current using vector control, VSC can independently control both active and reactive power. Reactive power can be controlled at each converter terminal regardless of the DC voltage level.
- Operation down to zero short circuit ratio. Converters can be operated anywhere in the AC network, as the operation of the converters does not require any short circuit power. This was one of the major drawback of thyristor based LCC system. It also provides the black start capability.
- No reactive power consumption for the operation of converters. Therefore huge capacitor banks are completely removed from the switchyard, thereby reducing the space requirement for the converter station.
- Instead of using converter transformers, ordinary transformer could be used for VSC station [3].

1.4 HVDC Configurations

The HVDC system can be configured in different ways [4]. The commonly used configurations are discussed in this section.

1.4.1 Monopolar HVDC system

It is further divided into asymmetric and symmetric monopolar system. An asymmetric monopole configuration involves operation of DC system with single positive voltage, while the return path of current is through the earth. The system involves only one set of conductor as shown in the figure 1.11, there is a continuous flow of current through the earth during the operation. In some cases, where earth return path is not possible due to highly congested areas or fresh water cable crossing, a metallic earth return path could be used. The losses increase in such arrangement due to resistance of metallic conductor.

Another configuration of monopolar system is symmetric monopolar type. In this system, each poles on both sides are connected to the high voltage cables, carrying half the rated power. This is illustrated in the figure 1.12. Each conductor in this configuration is subject to half the rated DC voltage and full rated current in opposite direction.

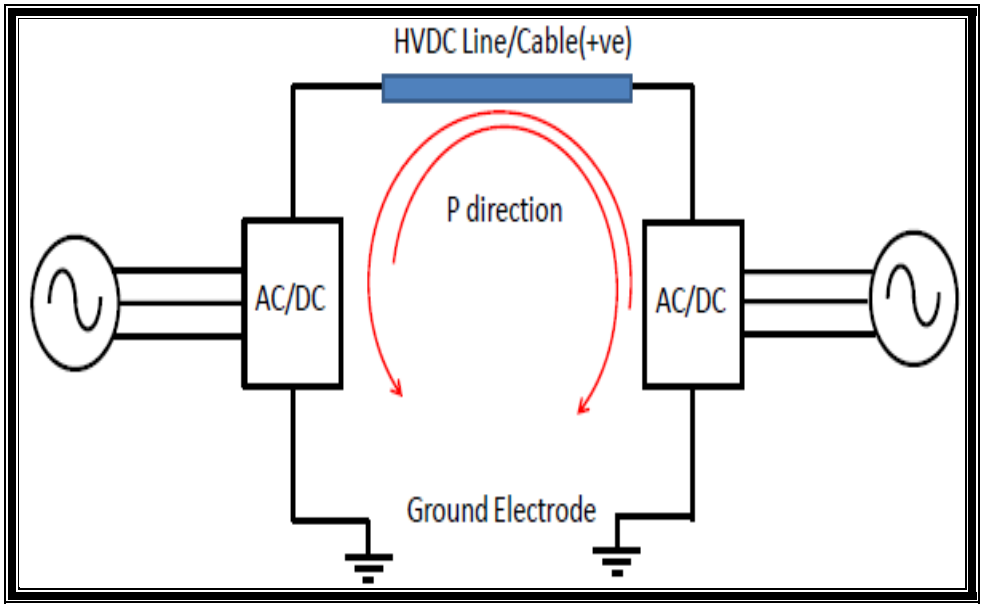

Fig. 1.11 Asymmetric Monopolar configuration

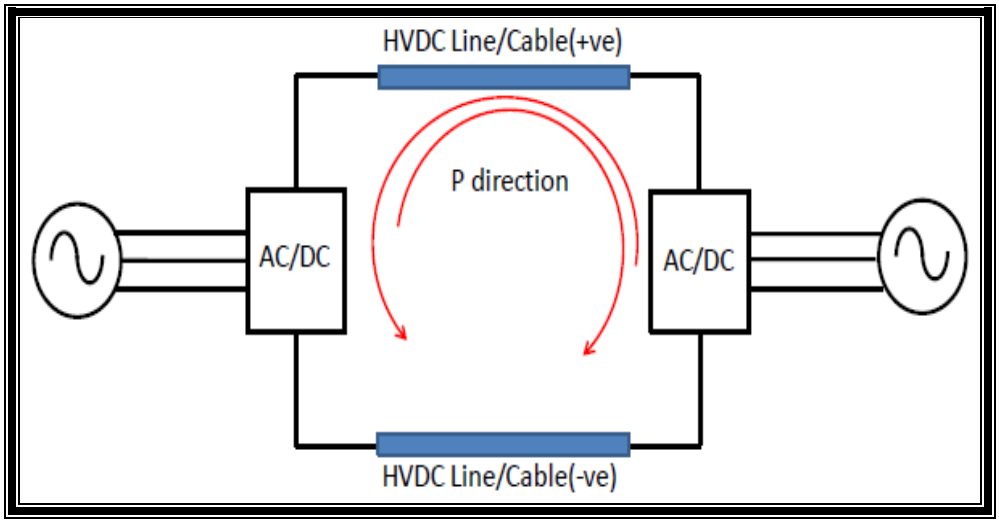

Fig. 1.12 Symmetric Monopolar configuration

1.4.2 Bipolar HVDC system

A higher power rating with greater reliability could be achieved using bipolar configuration. In a bipolar configuration, there are 2 poles, one as positive and the other as negative with respect to ground. Therefore, there are two sets of conductors each rated for full voltage. Current owing through the earth electrode in bipolar configuration is negligible during normal operating condition. The schematic and the current direction of a bipolar configuration is shown in the figure 1.13. A metallic return path could be provided for operation of the converter at its half rating during a fault in one pole.

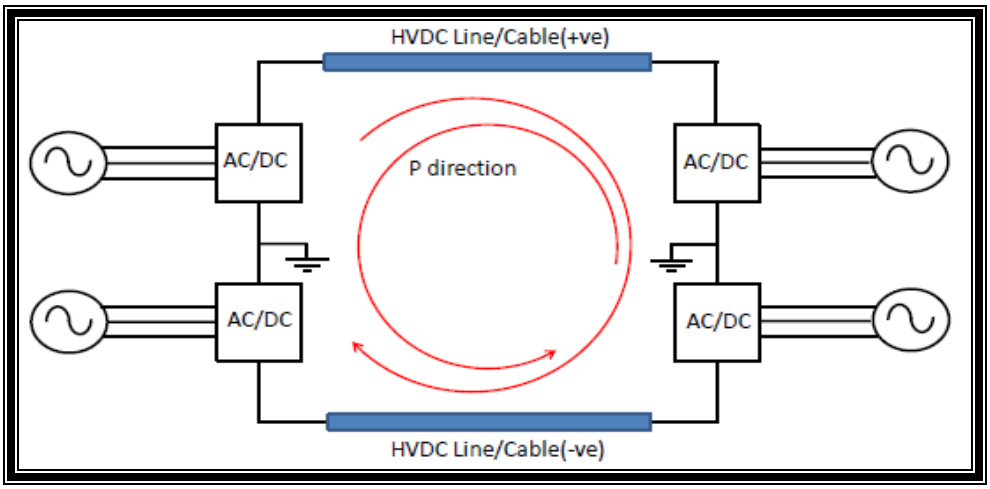

Fig. 1.13 HVDC Bipolar Configuration

1.4.3 Back-to-Back HVDC system

In Back-to-back HVDC system as shown in figure 1.14, there is no DC transmission line between the converters. Both rectifier and inverter are located at the same place. This configuration is used for the interconnection of two asynchronous AC networks.

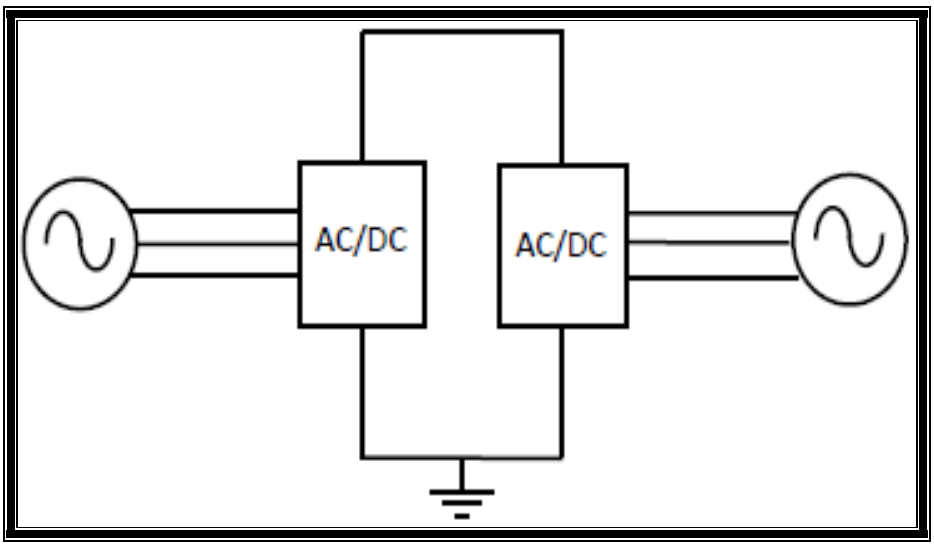

Fig. 1.14 Back-to-Back HVDC Configuration

1.5 Multi-Terminal HVDC System (MTDC)

Most LCC based HVDC systems currently existing are point-to-point with converter stations at both ends. The power transfer in such a configuration is achieved by manipulating the voltage magnitude of both the terminals and changing the voltage polarity. The need of flexible transmission capacity to balance the fluctuating power generation from renewable over wide geographical areas combined with corresponding potential benefits in a deregulated power market is expected to favour multi-terminal DC MTDC system with many converter terminals connected in a single grid. In such a system, the manipulation of voltage at each terminal become a tedious task and need complex control techniques and complicated switching and therefore LCC scheme does not favour multi-terminal system. However, with VSC technology, power reversal is now possible by changing the current direction with the voltage unaffected, thereby providing the ground for an MTDC grid.

A VSC MTDC system has many advantages over a two-terminal HVDC system, which includes increased transmission capacity, reduction in the cost and conversion losses, flexible control of

the power flow and enhanced reliability. MTDC configuration can be broadly classified into two based on the converter arrangement series configuration and parallel configuration.

1.5.1 Series Configuration

In series arrangement as shown in figure 1.15, one converter controls the current around the rated current, and is common for all converters, while other converters controls the power. LCC based system favours this configuration as they act as voltage source at DC side. This arrangement results in more losses, high insulation requirement and reduced reliability. A fault in one terminal of the system could results in complete MTDC to cut-off .

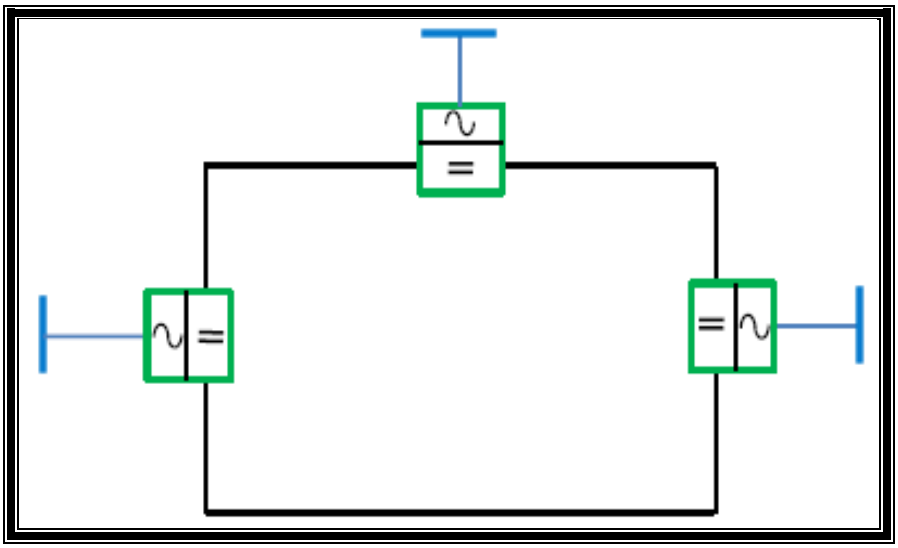

Fig. 1.15 Three terminal series MTDC system

1.5.2 Parallel Configuration

In this configuration, one converter sets the voltage, while others operate in power mode. The arrangement can be done in radial or ring configuration as shown in figure 1.16. The parallel configuration is always a preferred way of connection due to its reliability, as failure in one terminal will not affect the total MTDC system, provided that other terminals could carry the total power.

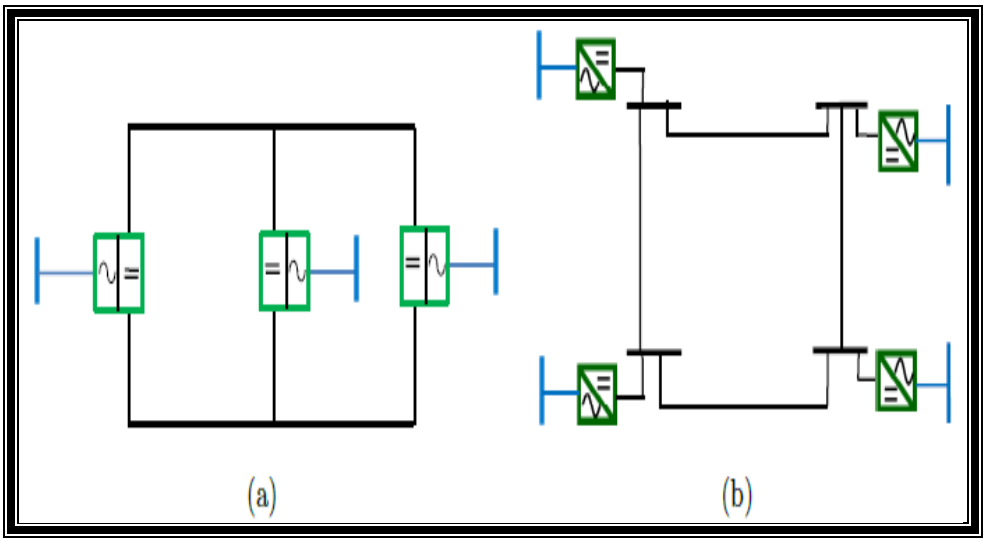

Fig 1.16 Parallel MTDC system

a-Radial configuration . b-Ring configuration

With the above two configurations many types of MTDC systems based on various application were proposed in the literature [6], some of which are listed below.

- **Double input single output(DISO) HVDC system** for offshore wind farms as shown in figure 1.17 - A 3-terminal double input single output HVDC system for interconnecting two neighbouring wind farms to an AC grid.

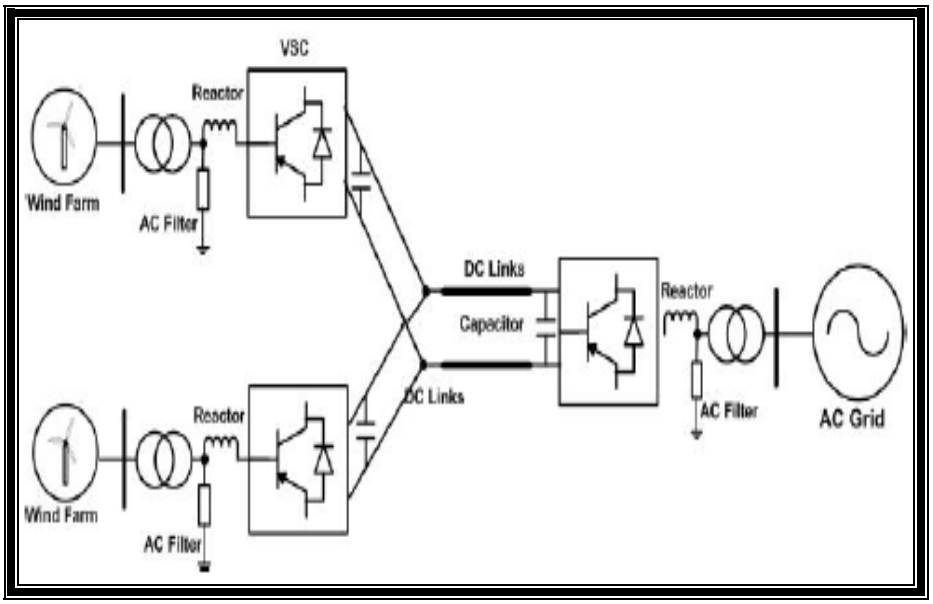

Fig. 1.17 Double input single output HVDC system

- **MTDC for oil and gas platforms** - A 3-terminal DC system of which a terminal for offshore wind farm is placed in between the oil platform terminal and onshore grid. Offshore wind farms can power up both oil platform and the onshore grid in this arrangement as shown in figure 1.18.
- **MTDC for urban distribution** - An HVDC network with multiple input-multiple output so that meshed ring shaped DC network is formed. The schematic is shown in figure 1.19.
- **CIGRE B4 MTDC Test Grid [8]** – CIGRE has proposed an MTDC grid consisting of several offshore wind farm converter terminals, oil platform terminals and onshore grid terminals operating with both Bipole and Monopole configuration.

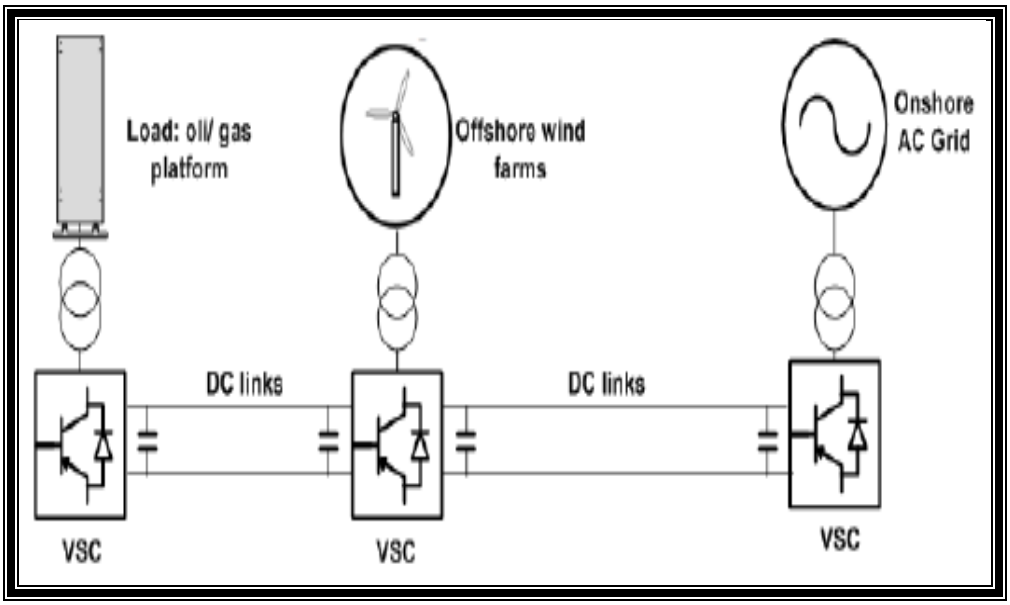

Fig. 1.18: 3-Terminal DC system for oil and gas platforms

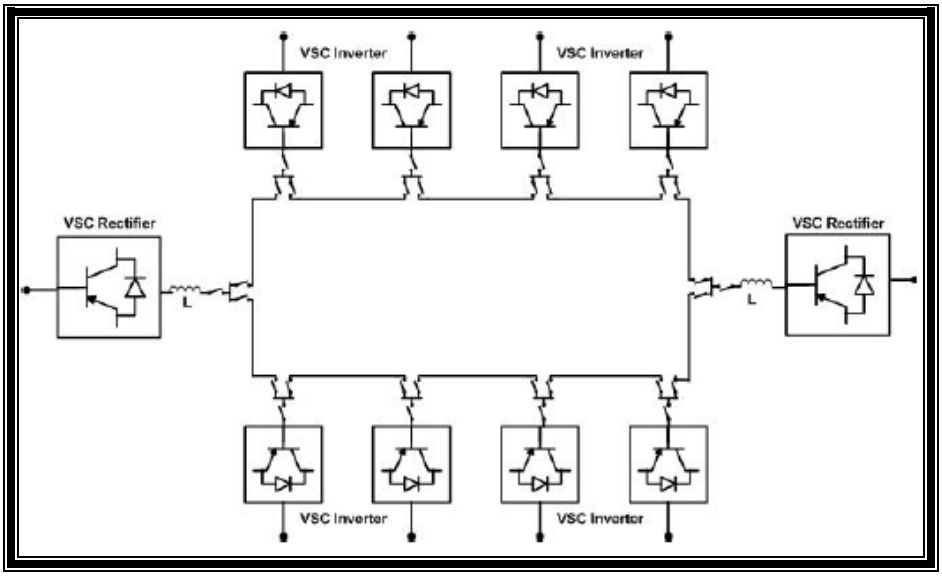

Fig. 1.19 Meshed ring shaped DC network

1.6 DC/DC Converters

A future HVDC grid is expected to emerge through a gradual development where point-to-point connections can later be connected into multi-terminal, meshed, configurations. A DC/DC conversion stage is required in such configuration due to following reasons.

- Two HVDC links operating at different voltage levels cannot be directly connected to each other. The exchange of power between these two networks need a DC/DC converter just like an AC transformer in an AC system.
- Two HVDC links operating with the same voltage but with different configurations. i.e , bipole or monopole, need a DC/DC converter for their interconnection.
- Power flow control through a particular section of the HVDC network.
- Interconnection of existing LCC based HVDC scheme with latest VSC based HVDC system can be done through a DC/DC converter.

The topology of DC/DC converter used in an HVDC grid varies for different applications. A high power DC interconnection could be classified according to the voltage ratio between two subsystems and is shown in Table 1.1 [5].

Table 1.1 HVDC interconnections

Nomenclature	Ratio
Low Ratio	$\frac{V_{DC,HV\ side}}{V_{Dc,LV\ side}} \leq 1.5$
Medium Ratio	$1.5 \leq \frac{V_{DC,HV\ side}}{V_{Dc,LV\ side}} \leq 5$
High Ratio	$\frac{V_{DC,HV\ side}}{V_{Dc,LV\ side}} \geq 5$

Wide range of DC/DC topologies including Buck converter, Boost converter, Buck boost converter, Cuk converter etc. are developed for low voltage applications. However, DC/DC converters for high voltage DC grid applications are not as mature as for low voltage applications. Based on the Table 1.1, a DC/DC converter used in an HVDC grid can be classified into two types.

- DC/DC Converters without galvanic isolation.
- Galvanically isolated DC/DC converters.

DC-DC converters play important role in dc grids in:

- ❖ interconnecting existing HVDC links (which have their local, optimized DC voltage level) into a dc grid .
- ❖ providing a connection between offshore and onshore dc systems (overhead lines have higher dc voltage).
- ❖ providing a connection to future dc cables, which will have higher dc voltage as cable technology improves.
- ❖ connecting with medium-voltage collection/distribution dc grids.

Chapter-II

Power Flow Controller for The Meshed DC Grids

CHAPTER TWO

Power Flow Controller for The Meshed DC Grids

2.1 Introduction

In this chapter, the concept of the dc power flow controller is explained. A simple 3-terminal system is described to give a good picture of the situation. The 3-terminal system has initially two transmission lines and it is upgraded to three lines. The 3-line 3-terminal system is introduced with the dc power flow controller and the benefits are evaluated using the region of operation.

New Energy is part of the renewable energy sources, their common features are: hidden dispersion, random , low energy density, Intermittent. Therefore their development and use subject to certain restrictions, technically there is a certain degree of difficulty. With a variety of large-scale renewable energy connected to the grid, the traditional power equipment, power grid construction and operation technologies in receiving ultra-large-scale renewable energy increasingly powerless, this must be the introduction of new technology, new equipment and the new network structure to meet the profound changes in the future energy landscape. HVDC technology based on voltage source converter (VSC) is an effective method which can solve the renewable energy parallel in grid, energy emergency support ,asynchronous interconnection of AC grid and other issues[7]. The three basic topology of DC grid are dendritic, ring, mesh network, and various combinations of the basic structure generate the complex DC Grid. Among them, the meshed network structure has better flexibility and redundancy to increase the reliability of the system and reduce the transmission distance, which is a firstly considered structure for the DC power grid construction in the future[8]. In recent years, in order to meet the DC grid development needs, many complex grid appears in the form of a few parallel lines between the two converter stations[9]. In this case, the converter station cannot control the power flow of the DC lines entirely by adjusting the terminal voltage and current, because the current of the line is determined by the resistance of the line to some extent. Thus, power flow control device for DC Grid is necessary, not only to achieve economic operation of the grid, but also to prevent the circuit of overload run in the fault condition.

2.2 DC Power Flow Controller

2.2.1 Description

The dc power flow controller is conceived as a mean to change the voltage at the dc terminals of a VSC station by a ratio M. The dc power flow controller can be modeled either as an ideal converter (Pin = Pout) or as some kind of power injection device. The dc power flow controller is modeled as an ideal converter whose input is VSC terminal voltage V_{VSC} and whose output is dc line voltage V_{line}.

The ratio M is the output-to-input voltage ratio of the ideal converter as given in Equation (2.1).

$$M = \frac{V_{line}}{V_{VSC}} \tag{2.1}$$

Among many requirements, the dc power flow controller has to be economical in order to be viable. It can be rated for only a fraction of the terminal converter ratings because line currents are very sensitive to voltage variations due to the low line resistances. Therefore, a variation of voltage of only 5%($\pm$2.5%).

2.2.2 Benefits

The 3-line system shown in figure 2.1(b) is upgraded with a dc power flow controller "M" as illustrated in figure 2.2. The ratio M is adjusted to force the HVDC grid to operate back with the same current values as with 2 lines figure 2.1(a).

A ratio of 0.989 makes the current in the link L_{12} almost zero, which reproduces the initial conditions. This situation is illustrated in figure 2.3(a). In the event that the wind farm (terminal station T_2) production reduces to 80MW instead of 100MW, the terminal station T_1 is able to increase its power injection by 20MW to compensate the reduction. However, it is required that the 20MW of extra power is transmitted via the L_{12}-L_{23} link and not L_{13} because line L_{12} is already at its nominal capacity. Then, the dc power flow controller is adjusted to 0.991 which forces the 20MW to flow via link L_{12}-L_{23} as shown in figure 2.3(b).

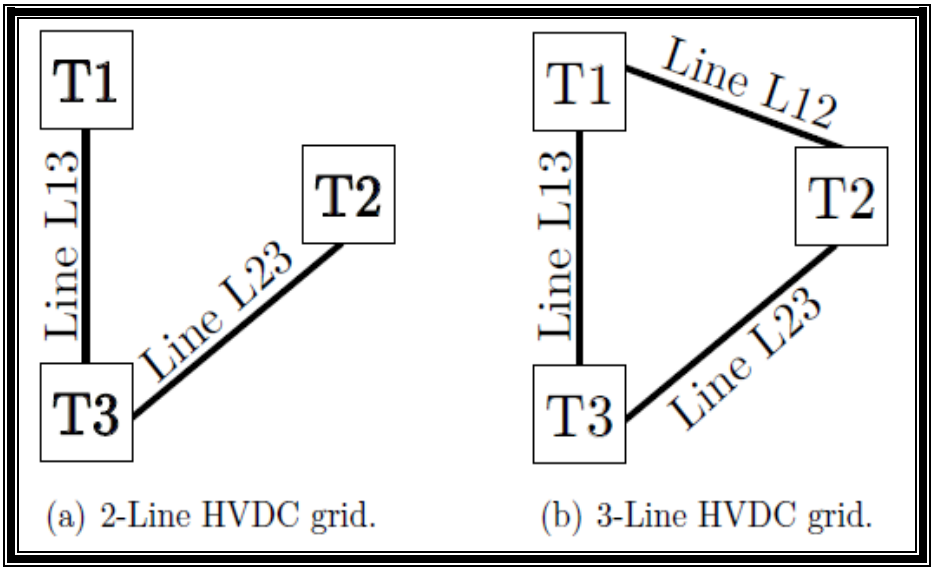

Fig 2.1 MTDC grid configurations with 3 terminal stations

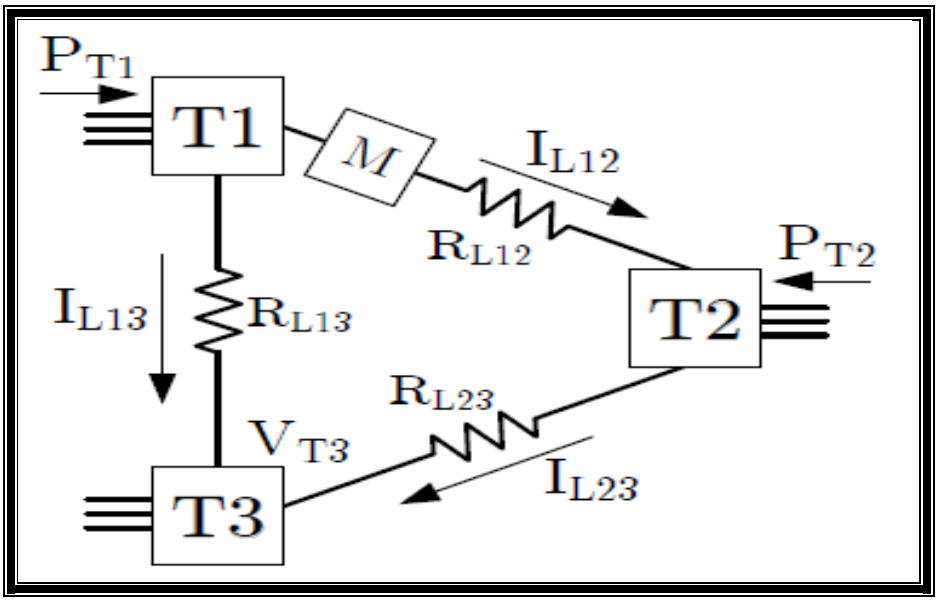

Fig. 2.2: 3-terminal HVDC grid with a dc power flow controller M

This simple example describes the operation and benefits of the inserted dc power flow controller on the HVDC grid. The extra contribution of 20MW by terminal station T_1 might appear to be unrealistic for an already installed converter with established power ratings. However, in the vision of a future HVDC grid, it is most likely that a terminal station T_1, for

example, will branch out to many converters and several dc power flow controllers may be installed. In that case, the requirement of additional power controllability would be served.

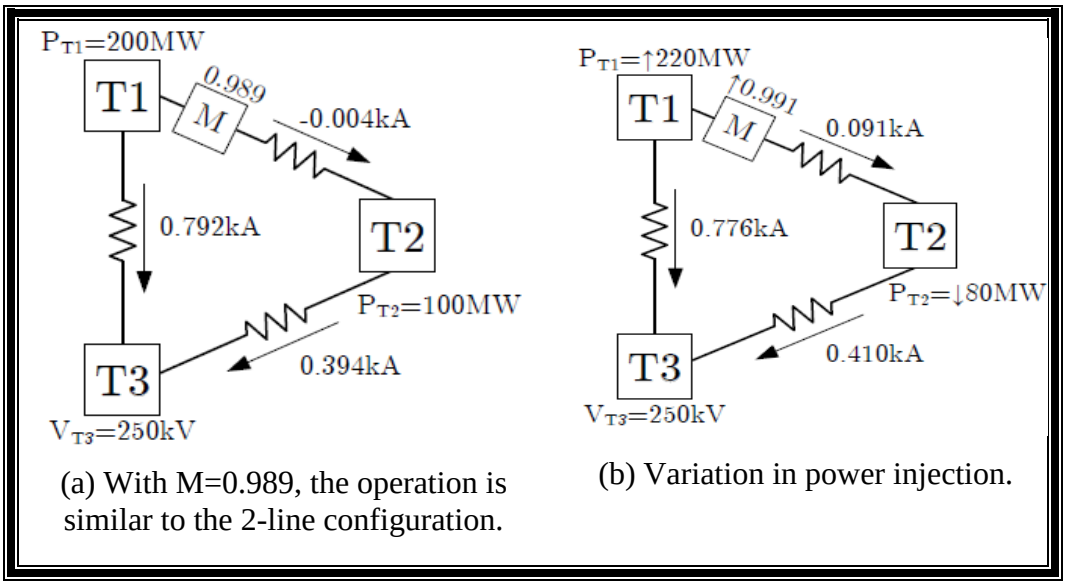

(a) With M=0.989, the operation is similar to the 2-line configuration.

(b) Variation in power injection.

Fig. 2.3 Example of the interaction with dc power flow controller

2.2.3 Region of Operation

As expected, the restricted region enlarges with the addition of the dc power flow controller. The dc power flow controller is inserted in the HVDC grid on line L12 between terminal stations T_1 and T_2 as in figure 2.2. The equation of the current in line I_{L12} becomes,

$$I_{L12} = \frac{MV_{T1} - V_{T2}}{R_{L12}} \tag{2.2}$$

where M is the output-to-input ratio of the dc power flow controller. The power of T1 and T2 are

$$P_{T1} = V^2{}_{T1}\left[\frac{1}{R_{L13}} + \frac{M^2}{R_{L12}}\right] + V_{T1}\left[\frac{-V_{T3}}{R_{L13}} + \frac{MV_{T2}}{R_{L12}}\right] \tag{2.3}$$

$$P_{T2} = V^2{}_{T2}\left[\frac{1}{R_{L23}} + \frac{1}{R_{L12}}\right] + V_{T2}\left[\frac{-V_{T3}}{R_{L13}} + \frac{MV_{T1}}{R_{L12}}\right] \tag{2.4}$$

The boundary of the region of operation is the dotted line in figure 2.4. This illustrates that the insertion of the dc power flow controller indeed enlarges the area offering more options to transmit power. The increase is significant compared to the system without M, it increases by 112% for the four quadrants.

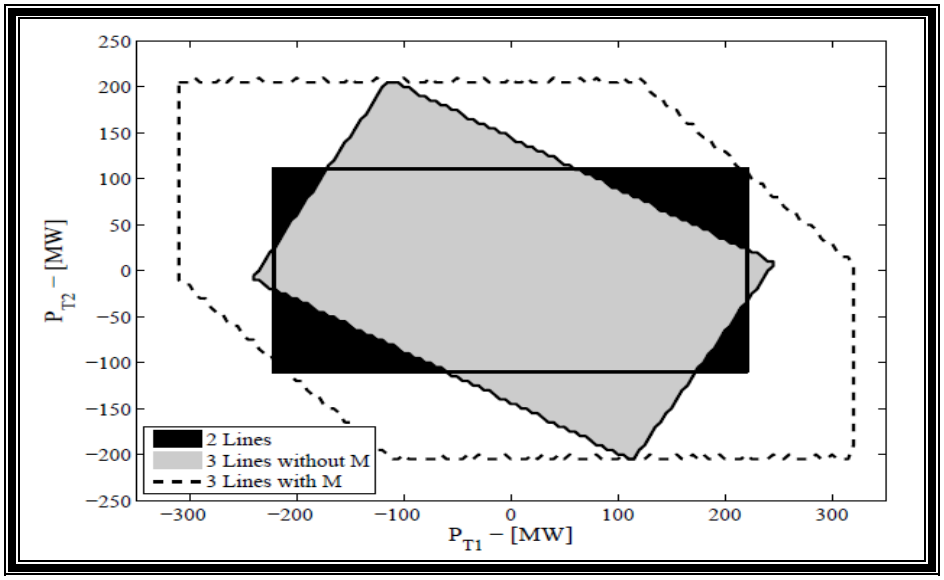

Fig. 2.4 Region of operation for the 3-terminal HVDC grid

Although the dc power flow controller is installed on one line, variations of M produce changes to all three lines as shown in figure 2.5. For the given P_{T1} and P_{T2}, 200MW and 100MW respectively, multiple operating points are possible depending on the value of M. Using Figure 2.5, if M is set to 0.975, transmission line L13 exceeds its current limits of 0.87kA. Therefore, by adjusting M to 0.99, all lines are within their respective boundaries.

This means that for a given P_{T1} and P_{T2} there is a range of M where all line currents are within their respective constraints.

Under certain power injections (P_{T1} and P_{T2}), there are always one or multiple lines that exceed their limits regardless the range of M.

The lines responsible for the limits of the region of operation are shown in Figure 2.6. The lines responsible for the boundary are identified and in the event of concurrent exceeding lines, an "X" is used.

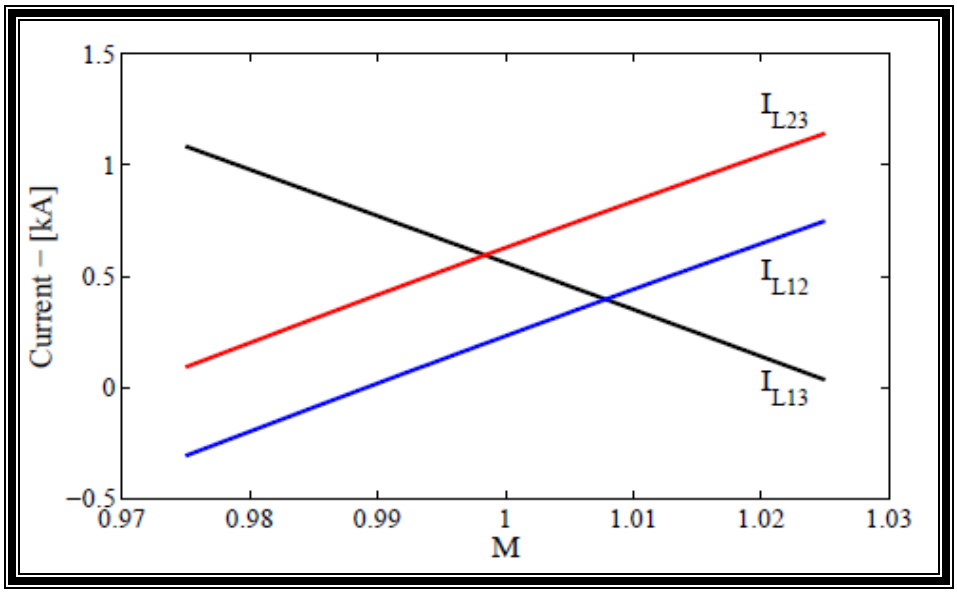

Fig. 2.5 Line current variations with respect to M with PT1=200MW And PT2=100MW for the 3-terminal 3-line HVDC grid

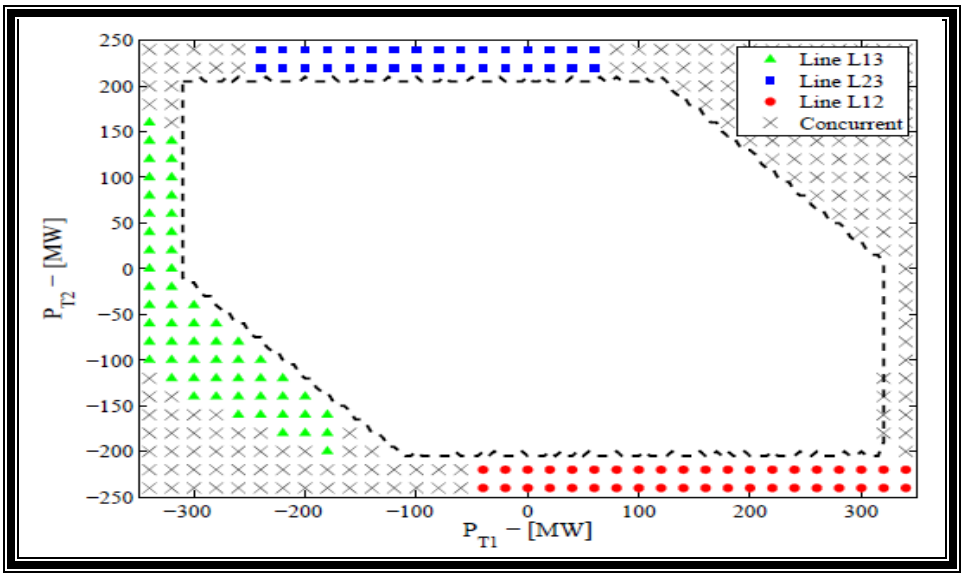

Fig 2.6 Boundary analysis line limits for the 3-terminal 3-line HVDC grid

2.2.4 Current Sensitivity

As stated previously, line currents are very sensitive to the ratio M. As shown in figure 2.5, a variation of only 1% in the ratio M produces a change of around 20% in the three currents. More precisely, the current sensitivity can be calculated by doing the partial derivative of the current lines. The results are shown in Equations (2.5), (2.6) and (2.7).

$$\frac{\partial I_{L13}}{\partial M} = \frac{1}{R_{L13}}\frac{\partial V_{T1}}{\partial M} - \frac{1}{R_{L13}}\frac{\partial V_{T3}}{\partial M} \tag{2.5}$$

$$\frac{\partial I_{L23}}{\partial M} = \frac{1}{R_{L23}}\frac{\partial V_{T2}}{\partial M} - \frac{1}{R_{L23}}\frac{\partial V_{T3}}{\partial M} \tag{2.6}$$

$$\frac{\partial I_{L12}}{\partial M} = \frac{M}{R_{L12}}\frac{\partial V_{T1}}{\partial M} - \frac{1}{R_{L12}}\frac{\partial V_{T2}}{\partial M} + \frac{V_{T1}}{R_{L12}} \tag{2.7}$$

Since the dc voltage of the voltage regulator terminal station, V_{T3}, is constant, its partial derivative with respect to M is zero ($\frac{\partial V_{T3}}{\partial M} = 0$) . The power equations of terminal stations T1 and T2, Equations (2.3) and (2.4), are used to find numerically the value of $\frac{\partial V_{T1}}{\partial M}$ and $\frac{\partial V_{T2}}{\partial M}$. Those calculations for P_{T1} =200MW and P_{T2}=100MW give a slope $\Delta I_L/\Delta M$ around the operating point M=1 of (-21.03 kA), (21.03 kA) and (21.13 kA) for I_{L13}, I_{L23}, I_{L12} respectively. Those numbers also match the calculated slopes using the linear fitting curve of figure 2.5. This analysis confirms the high sensitivity of the line currents with respect to the dc power flow controller. Therefore, it justifies the need of only a small voltage variation. It can be noted that the current change is almost linear. In the event where more degrees of freedom would be required, the addition of more modules can result in an increase of the possibilities.

2.3 Comparative study of various kinds of Power Flow Controller

There are mainly four DC power flow control equipment researched at home and abroad, namely variable resistor, DC transformer, current flow controller and series voltage source [7],[10]. The following are brief introductions of those four kinds of controllers, and compare their advantages and disadvantages.

2.3.1 Variable Series Resistor

We know that the DC current flowing through the DC grid is determined by the line resistance, so even a very small change can have a significant effect. Therefore, the DC current of the grid can be controlled by simply adding additional resistance to the line of least resistance. A basic structure of variable series resistor, as shown in figure 2.7 [10]. In this method, each resistor switching into the DC line to complete the line current regulation, in order to achieve the effect of power flow control.

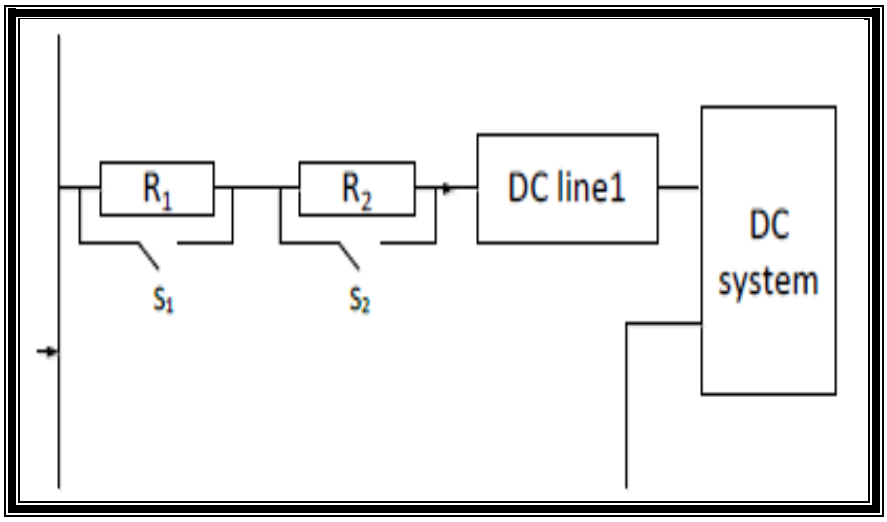

Fig.2.7 Variable Series Resistor control circuit current

In figure 2.8 another detailed topology [7].This topology consists of two anti-parallel resistors connected in parallel to the positive and negative poles. The meaning of the anti-parallel resistors is to keep the balance of positive and negative transmission effects from the device. P_1, P_2 access to positive electrode, and N_1, N_2 access to negative electrode. The inductor series in the line is for smoothing and mitigate the impact of switching equipment. Bi-directional IGBT can achieve two-way power flow. The diodes connected with in series is to withstand the reverse voltage, because the IGBT can hardly withstand the reverse voltage. The equivalent resistance accessed can be controlled by the control of the switch, the principle formula is as follows:

$$R_{ave} = \frac{T_{OFF}R + T_{ON} \cdot 0}{T} = (1 - \sigma)R \tag{2.8}$$

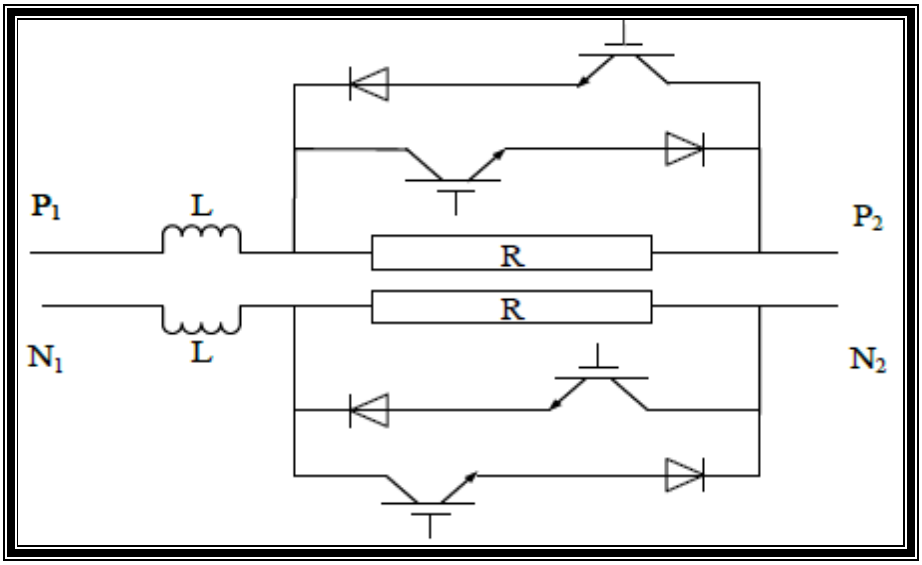

Fig. 2.8 Topology of the Variable Series Resistor

Under normal circumstances, it depends on several factors when the device can be applied in the power system. One is that the IGBT of the devices suitable for the trend reversal of the VSC. The second is the average resistance value of the resistor can be a smooth change to the reference value. Because of its simple structure, it can easily access to an existing project. But the series resistance consume additional power loss, so it is not suitable for the economic operation.

2.3.2 DC Transformer

DC transformer not only can be used to connect the DC grid with different voltage levels, but can also be used in the grid with the same voltage level. A typical DC transformer is shown in figure 2.9. In figure 2.10 show a general model of a DC transformer [10]. In this model, the primary side is current source I_{SR} , paralleled with a capacitor C_E . The secondary side is voltage source U_{SR} and series with the equivalent inductance L_E , L_1 and C_2 as the real component of the DC transformer is also included. The output voltage of the secondary side U_{SR} can be individually controlled. According to the principles of the transformer, I_{SR} can be calculated according to the formula as follows

$$I_{SR} = \frac{U_{SR} I_{d2}}{U_{d1}} \tag{2.9}$$

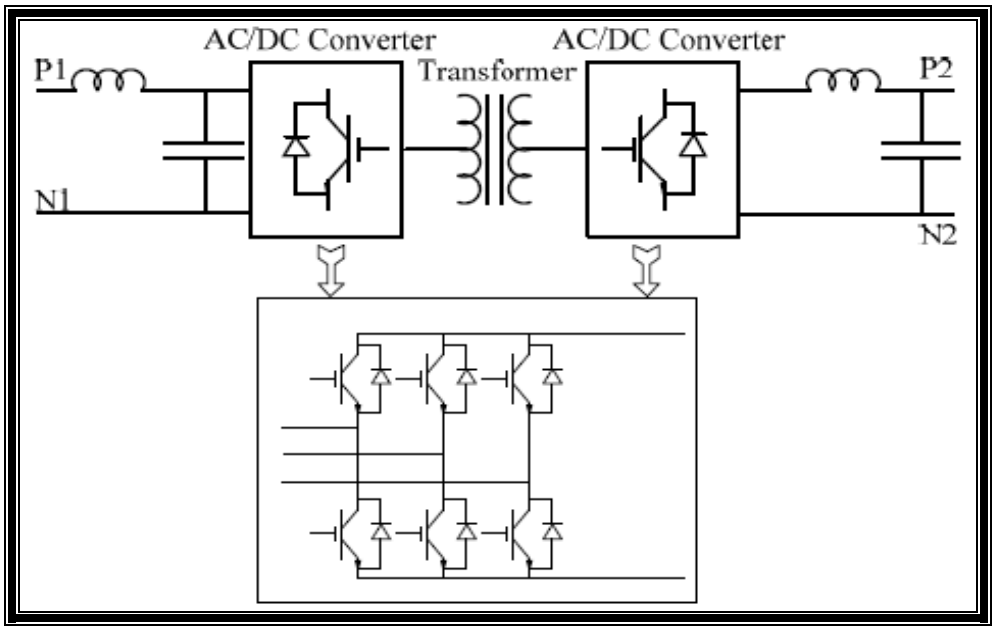

Fig.2.9 A topology of DC transformer

In order to achieve complete control of the injected electrical energy, DC transformer will adjust the output voltage. Control method of DC transformer's power flow is shown in figure 2.11,which is composed of two parts. The first part is power flow regulation. There are two input signals, the expected current of DC line I_{dref} and the actual current I_d.Thereafter, the error current signal is sent to a PID controller. Another part is used to generate the reference voltage, which uses the received signal adjustment and generating the reference voltage of U_{SR}.

In this session, U_0 is the rated voltage of the DC grid, so as to ensure the normal operation of the DC transformer.

In fact, the function of DC transformer could easily be presented by a unit shown in figure 2.12 and **(K)** is the ratio of the voltage between the primary and secondary side.

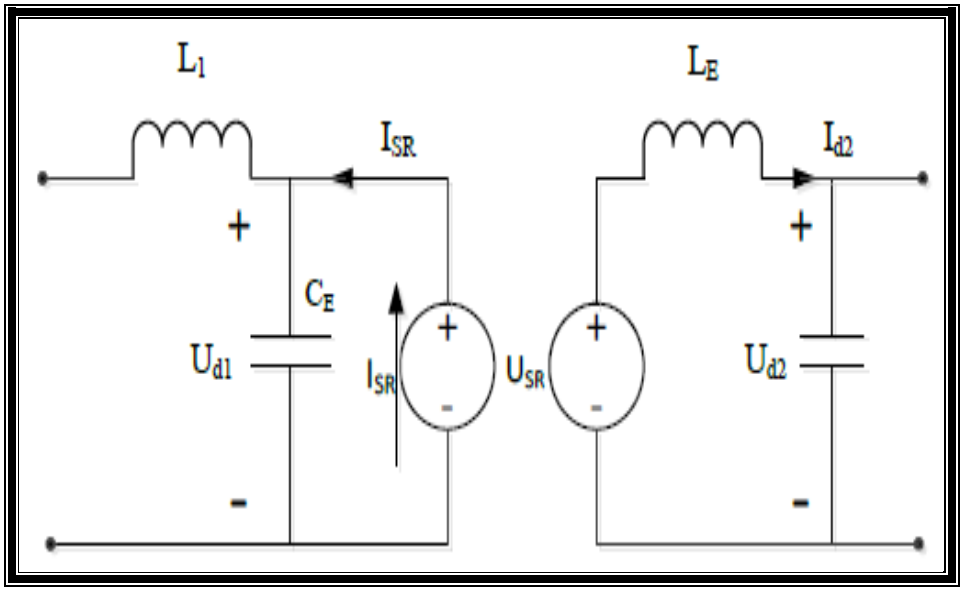

Fig.2.10 General Model of DC transformer

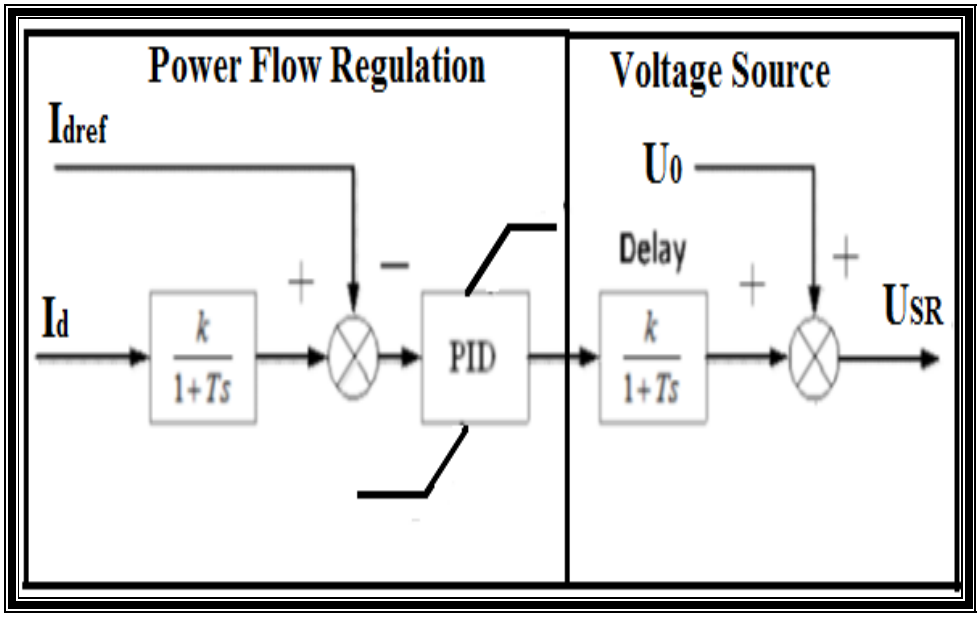

Fig.2.11 Power flow control diagram of DC transformer

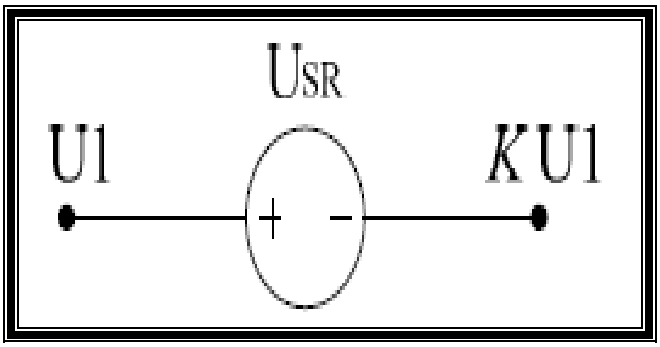

Fig.2.12 The unit to represent DC transformer

Due to the voltage of DC grid has no uniform standard, there is various voltage levels of the DC grid, so the DC transformer is essential equipment. so far the DC converter has no application in the DC transmission, but there will be a lot of DC transformer applications in the future.

DC transformer needs to achieve the following functions:

- high transformation ratio.
- controllable.
- ladder-type ratio.

To connect different voltage levels DC system; can be connected to different types of inverter; power balance between DC system poles; controllable bidirectional flow direction; low loss, low cost, small size; has a certain capability of current fault withstand .

2.3.3 Series Voltage Source

A novel topology for a series voltage source is proposed as shown in figure 2.13. This series voltage source contains two entirely equal components with regards to the balance of the positive and negative polarities. An AC source is connected to the AC side of an AC/DC converter through a transformer. This transformer is used to provide isolation between the AC source and the DC grid. This transformer steps up the voltage, leading to reduction of the injected current in the AC source. The AC/DC converter uses a typical 6 pulse voltage source converter, which is responsible to maintain the voltage of the capacitor, U_d.

A DC/DC converter is used to regulate the DC output of this device, ΔU, to change the power flow of the DC grids. The topology of the DC/DC converter is a typical H bridge. An inductor, L, is connected in series to smooth the current. The DC cable current flows through the DC/DC bridge and the capacitor, which might filter this current, and enters into the AC source via the AC/DC converter. The scheme of control system is shown in figure 2.14, and the PWM firing part that is prevalent in practical project. It is easily seen that this control system is compose of power flow regulation and voltage reference generator.

For the power flow regulation, there are two inputs, I_{dref} and I_d, which represents the reference current and the measured current of the DC transmission line to be controlled. The error signal of the current is fed to a PID regulator.

Then, in the voltage reference generator, an inertia block, which mimics the delay in practical situation, would postpone the signal. In addition, The output, ΔU_{ref} represents the signal entering into the PWM block to regulate the output of voltage, ΔU.

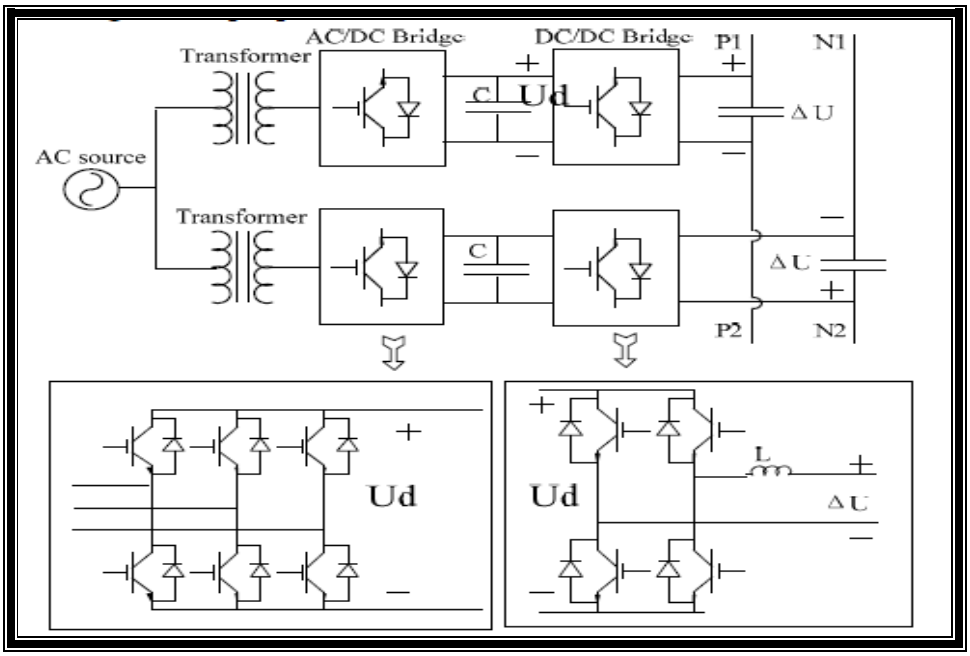

Fig.2.13 series variable voltage source

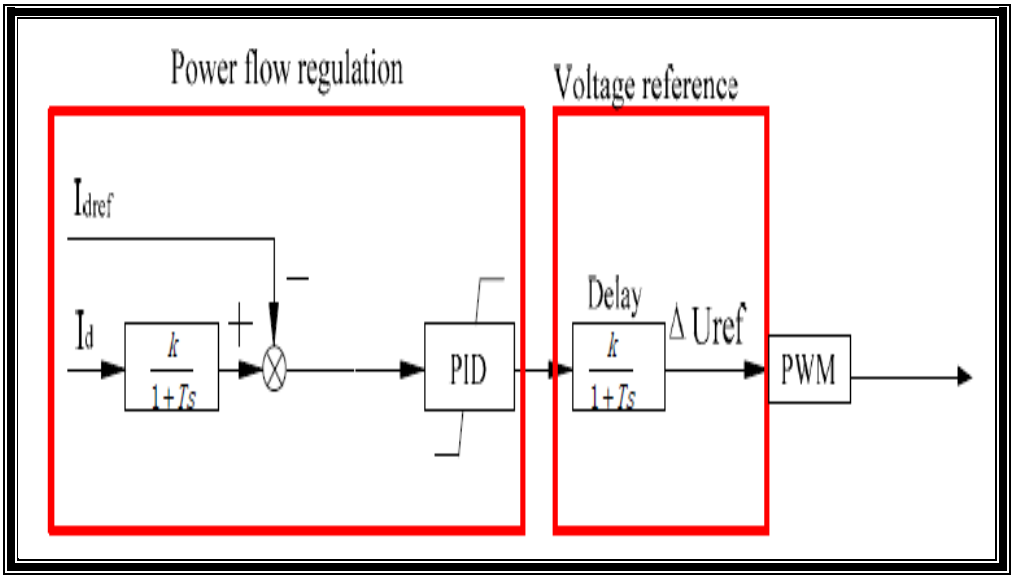

Fig.2.14 the control scheme of series variable voltage source

The DC/DC converter can rapidly response to variation of voltage reference with fewer harmonic. Also, the set of AC source and transformer is available in practical.

It is usually installed near a converter station for conveniences, thus, the AC source is easy to be approached, no matter single phase or three phases. The step up transformer benefits a wider range of the operation currents, by decreasing the current in the AC source side.

In this type the principle is similar, which is taking the energy from AC system into DC voltage source through rectifier and connect in series with the DC line, enabling power flow control of the DC grid [12]. This method is actually replacing the series resistance of a voltage source, so as to achieve better control. The form of series voltage source access into the DC grid shown in figure 2.15.

Figure 2.16 shows the specific topology of the series voltage source. This model includes two identical modules to balance the positive electrode and the negative electrode lines. AC power is connected to the AC side of the converter via a transformer, which is used to isolate the AC and DC power grids, and can also reduce the current injected into the AC system.

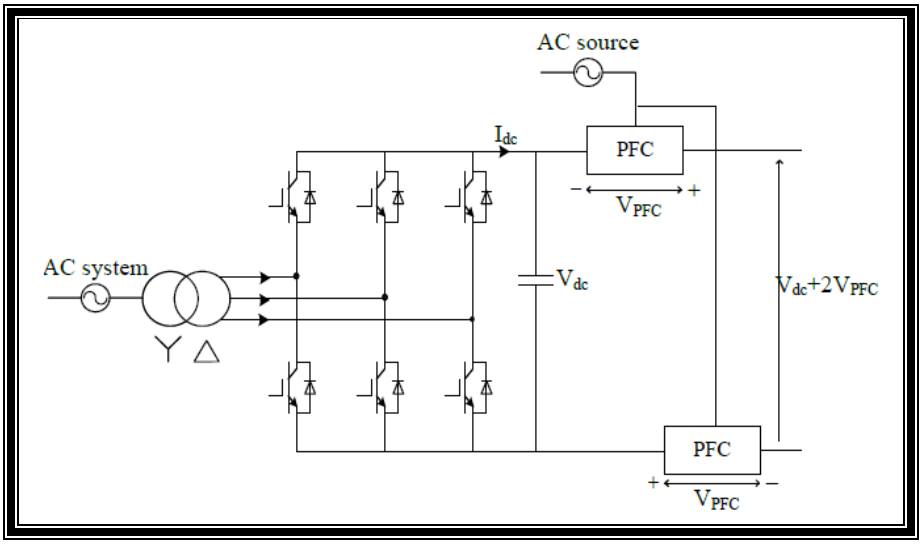

Fig.2.15 Series voltage source access in the DC grid

AC/DC converter using a typical 6-pulse voltage source converter to maintain the voltage of the capacitor. DC/DC converter is used to adjust the inverter's output voltage so that the voltage accessed to the DC grid will finally meet the power flow control requirements. The DC/DC converter a four-quadrant chopper, as shown in figure 2.16.

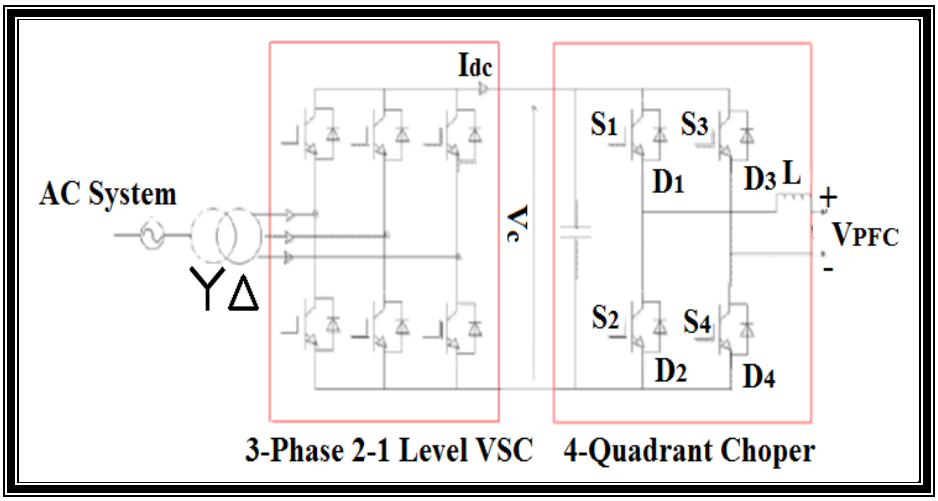

Fig.2.16 Topology of the series voltage source

The control system of the device shown in figure 2.17, the control system includes power flow regulator and a reference voltage generator. Two input of the regulator are the reference current I_{dref} and the actual current I_d Then generates a reference voltage V_{PFCref} finally into the PWM

module, and the DC/DC converter will be adjusted quickly. It is worth mentioning that there usually has single-phase or three-phase AC power system and transformer nearby the converter station, so the device can be easily implemented in the practical.

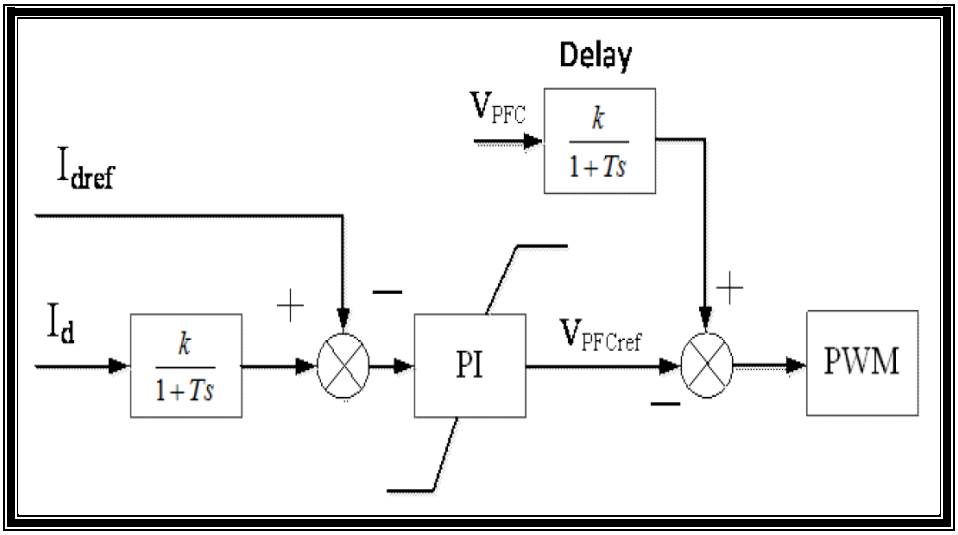

Fig.2.17 The control method of the series voltage source

2.3.4 Current Flow Controller(CFC）

There are two topology of direct current power flow controller (CFC) [7], one is shown in figure 2.18. The two converter modules in this topology are connected in series with two DC lines. The voltage of each converter module is formed from pulse width modulation by the power switching devices (typically IGBT), to control the current flow in the conductor. Since the device is actually only play a role in the rational allocation of direct current, so there is no power loss in theory. In practice, however, there will still be a corresponding power switching and conduction losses.

In figure 2.19 shows another topology of CFC applied in the DC grid [11]. CFC can take energy from other DC branch point, so the power electronic devices don't need to withstand the high DC voltage, nor need a converter transformer. DC current is very sensitive to the change of DC voltage, and the average voltage on branch 1 and 2 introduced by the CFC is much smaller compared to the DC voltage. The capacitor voltage is also smaller, and the voltage which power

electronic devices in the CFC have to withstand is closely related to the capacitor voltage, so the CFC required less number of power electronics. Thus, the investment of CFC is less. Meanwhile, the less number of electronic devices means low running loss, which is favorable to the long-term economic operation.

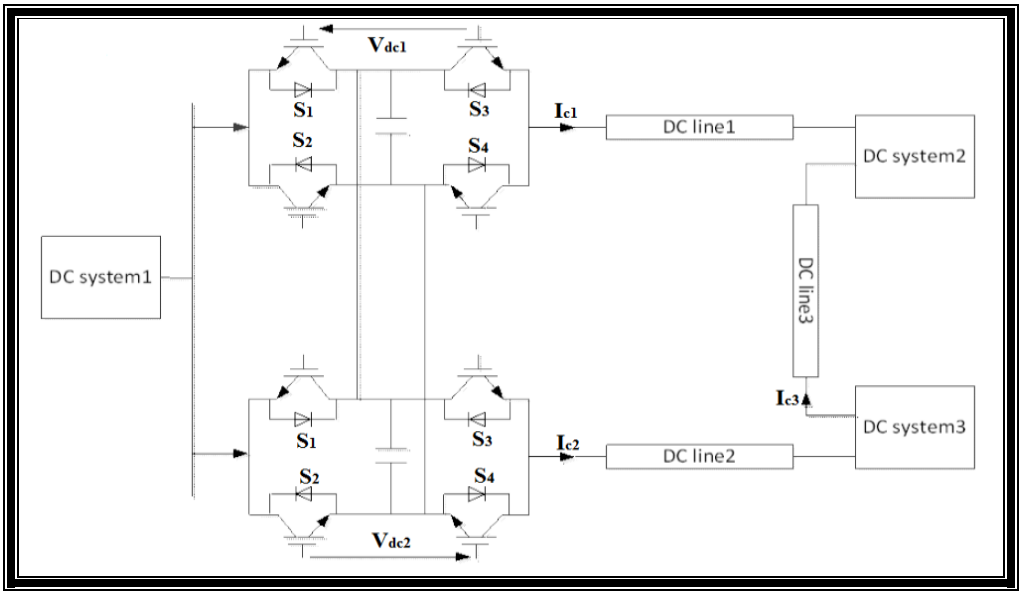

Fig.2.18 Current flow controller model one

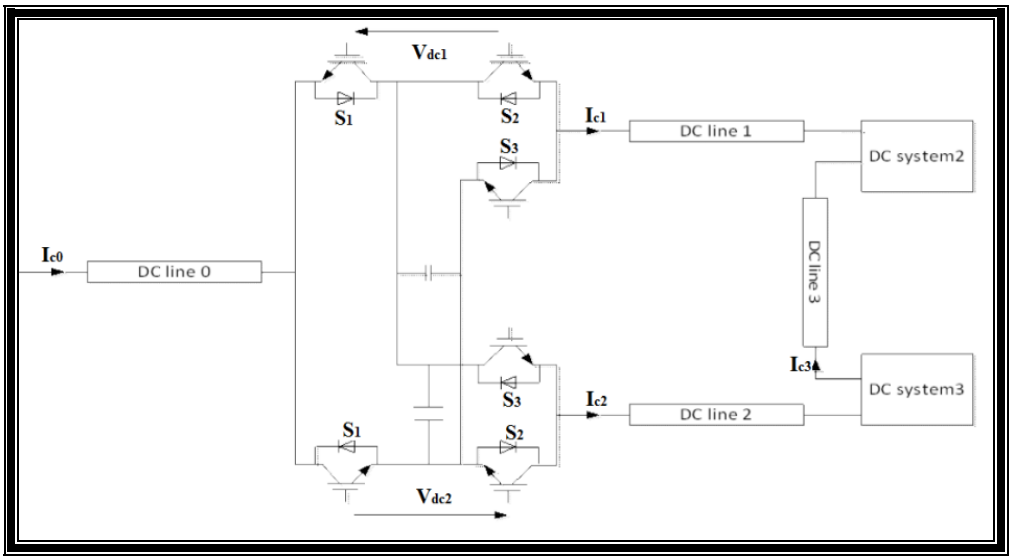

Fig.2.19 Current flow controller model two

2.4 Model derivation of Current Flow Controller

2.4.1 DC grid under study

The following work can be applied to any meshed DC grid. For this study, a 3 terminal meshed grid with 3 nodes is used, which can be seen in figure 2.20. The DC grid is a symmetrical monopole, but this work considers only one half in order to keep the symmetry using a single power flow device. CFC is assumed to be located in node 1. Nevertheless, it could also be placed in node 2 or 3, given its bi-directionality.

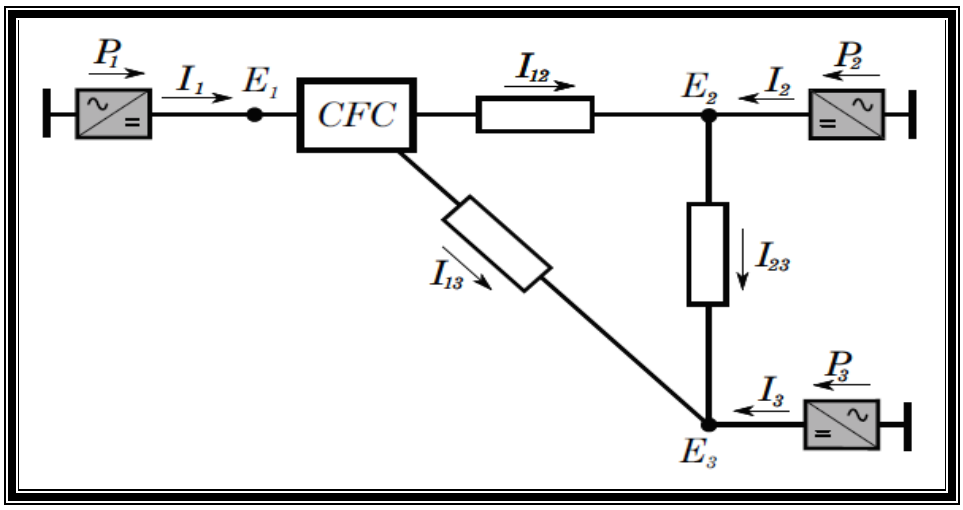

Fig.2.20: 3-terminal DC grid with CFC located in node 1

2.4.2 CFC under study

The CFC under study is a DC/DC converter connected between two cable lines. Its operation consists on exchanging power between these lines in order to regulate DC currents. It extracts power from one cable and it feeds the other. Thus, it applies positive voltage on one line and negative voltage on the other one. The converter is made of two H-bridges with 4 IGBTs and their antiparallel diodes figure 2.21(a). For this specific study, a simplified topology also presented is used. The two capacitors of the H-bridges are merged into a single one and two IGBTs are removed from the model leading to the converter depicted in figure 2.21(b). The converter has bidirectional capability, it can deal with all possible current configurations. There are 6 possible combinations of currents I_1, I_{12} and I_{13} going in or going out of the converter.

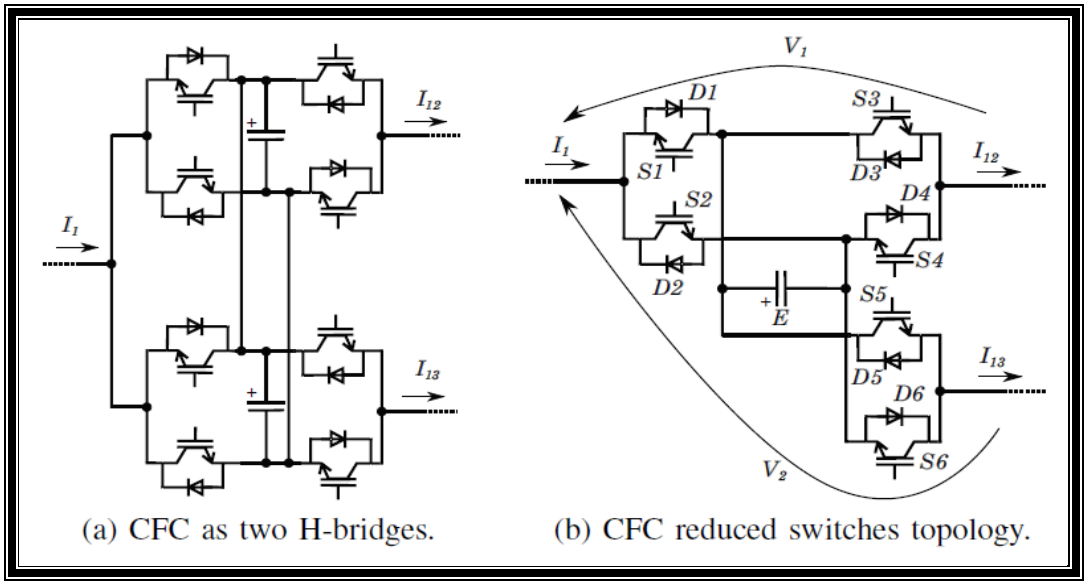

Fig.2.21. CFC topologies

The current direction of each branch defines the available switches to operate. If I_1, I_{12} and I_{13} are positive, the devices that are able to conduct given the current direction are: Diodes D1, D4 and D6 and switches S2, S3 and S5. When the switch of one branch is **ON**, the corresponding available diode of the same branch cannot be conducting as it is reverse-biased since the capacitor voltage is always positive. Therefore, if S2 is conducting, D1 is reverse-biased and consequently in open state.

2.4.3 Operation principle

The operation principle of the CFC contain from two current flow scenarios are considered. The first one assumes that I_1 is going out the CFC and I_2 and I_3 are entering. The second one considers the currents in opposite direction compared with the first case. This analysis can be extended to the rest of possible current configurations.

In order to share power within the two lines, the converter capacitor should be charged and discharged continuously. Only 4 states (two pairs) from the group of 8 for each current configuration are used to control the device in such conditions: (b,c,f,g) for positive current scenario and (j,k,n,o) for negative current scenario. Those states are the ones which enable the

charge of the capacitor using one current line and the discharge employing another one. They are used in pairs of two states, one state charges the capacitor and the other discharges it.

One pair limits the current through one line and the other pair increases current through the same line. Both pairs have a positive voltage in the capacitor, however one pair applies positive voltage in one line and the other applies negative voltage in the same line (c with g, b with f). Both pairs can be seen in figure 2.22 and figure 2.23 for each scenario. The following analysis is performed considering the first scenario with positive currents. It must be noticed that the difference between the two states of the same pair is only the switch S2. Using the commutation of that switch is possible to increase one line current (I_{12}) and decrease the other (I_{13}) (Pair A).

If the reverse effect wants to be achieved, the procedure should be changing the states of switches S3 and S5 and keep operating with S2, what is equivalent as working with Pair B. Below, the analytical analysis of the converter is performed for the two pairs of states presented before. Then, the conclusions and the average model can be extended to the whole range of current configurations. The duty cycle of switch S2 for pair A and B are defined as (2.10).

$$D_{s2A} = \frac{t_{s2A}}{T} \quad , \quad D_{s2B} = \frac{t_{s2B}}{T} \tag{2.10}$$

The average current through the capacitor can be calculated as a function of the line currents and the duty cycles for each pair (2) and (3).

$$\bar{I}_{cA} = \frac{1}{T}\int_0^T i_{cA}dt = \frac{1}{T}\left(-I_{12}t_{s2A} + I_{13}(T - t_{s2A})\right) = -I_{12}D_{s2A} + I_{13}(1 - D_{s2A}) \tag{2.11}$$

$$\bar{I}_{cB} = \frac{1}{T}\int_0^T i_{cB}dt = \frac{1}{T}\left(-I_{13}t_{s2B} + I_{12}(T - t_{s2B})\right) = -I_{13}D_{s2B} + I_{12}(1 - D_{s2B}) \tag{2.12}$$

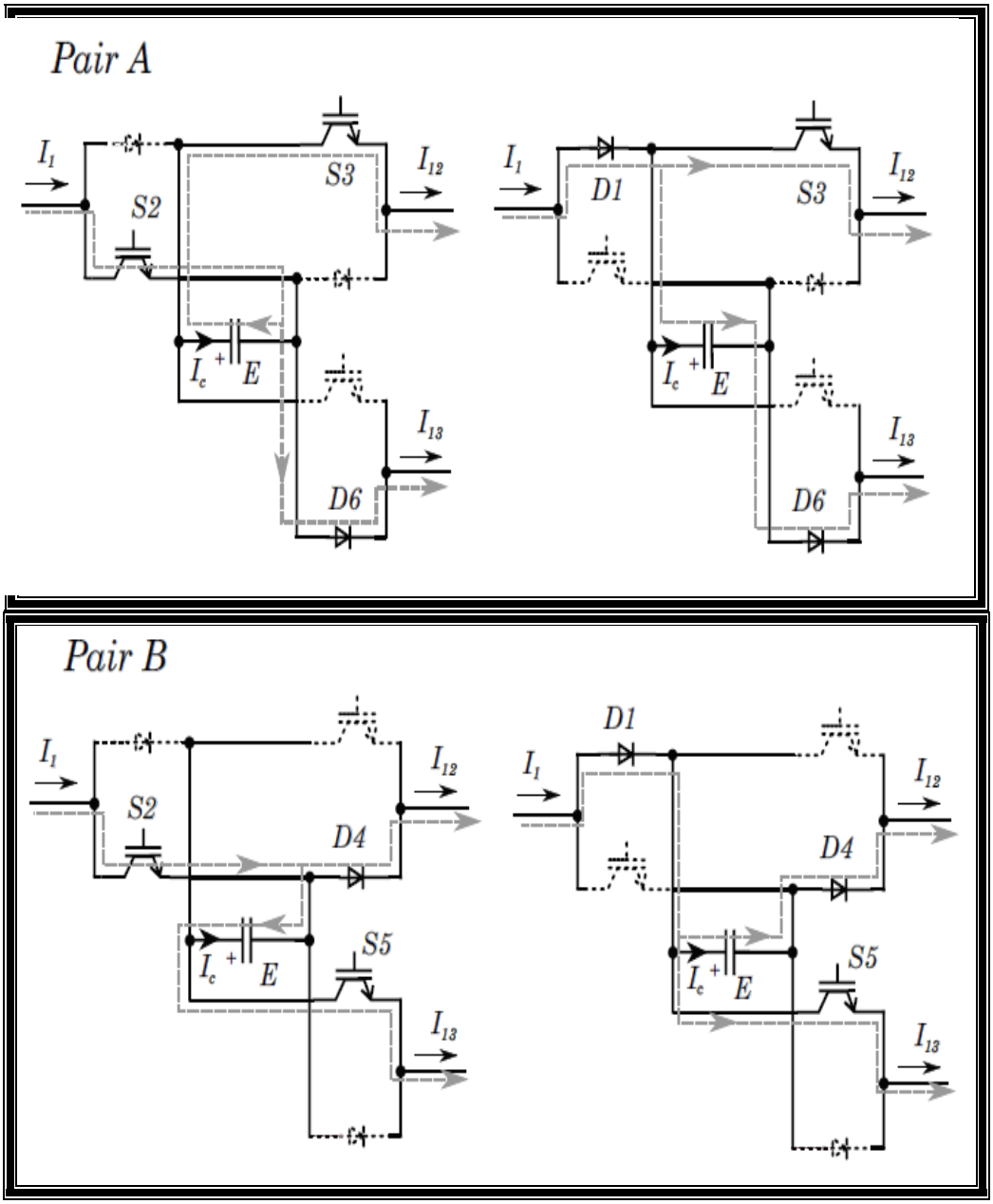

Fig.2.22. Pair A and B

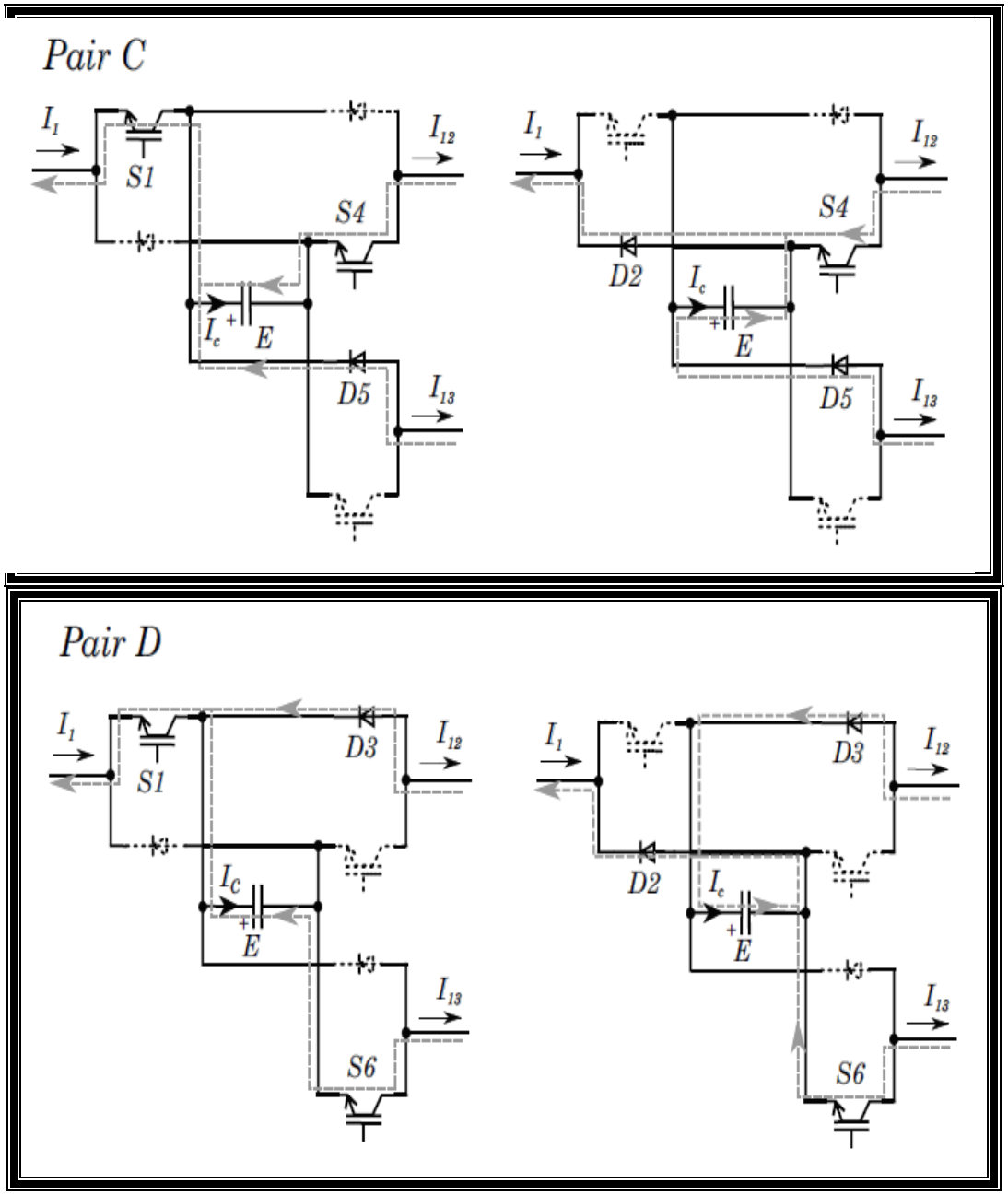

Fig.2.23 Pair C and D

In order to ensure that the average capacitor voltage is constant in steady state, both capacitor currents from equations (2.11), (2.12) must be zero. This fact shows that the duty cycle for each pair is going to be determined by line currents relation. The relation derived from equations (2.11) and (2.12) is shown in expression (2.13).

$$D_{s2A} = \frac{I_{13}}{I_{12} + I_{13}} = \frac{I_{13}}{I_1} \quad , \qquad D_{s2B} = \frac{I_{12}}{I_{12} + I_{13}} = \frac{I_{12}}{I_1} \tag{2.13}$$

In order to gather both duty cycles in the whole average model, a new one is defined as a relation between DC currents (2.14).

$$D = \frac{I_{12}}{I_1} = D_{s2B} = (1 - D_{s2A}) \tag{2.14}$$

The average voltages applied by the CFC with I_1, I_{12} and I_{13} positive are (2.15), and (2.16) working with pair A.

$$\bar{V}_{1A} = \frac{1}{T}\int_0^T v_{1A}dt = \frac{1}{T}(\bar{E}t_{s2A}) = \bar{E}D_{s2A} = (1 - D)\bar{E} \tag{2.15}$$

$$\bar{V}_{2A} = \frac{1}{T}\int_0^T v_{2A}dt = \frac{1}{T}(-\bar{E}(T - t_{s2A})) = -(1 - D_{s2A})\bar{E} = -D\bar{E} \tag{2.16}$$

And (2.17) and (2.18) working with B.

$$\bar{V}_{1B} = \frac{1}{T}\int_0^T v_{1A}dt = \frac{1}{T}(-\bar{E}(T - t_{s2B})) = -(1 - D_{s2B})\bar{E} = -(1 - D)\bar{E} \tag{2.17}$$

$$\bar{V}_{2B} = \frac{1}{T}\int_0^T v_{2B}dt = \frac{1}{T}(\bar{E}t_{s2A}) = \bar{E}D_{s2B} = D\bar{E} \tag{2.18}$$

The same analysis can be done considering currents I_1, I_{12} and I_{13} negative. In that scenario, the available switches and diodes to conduct are: S1, S4, S6, D2, D3 and D5.

The difference between the two states of the same pair is also the switch state that gathers all the current from two lines, S1. The voltage applied on each line is positive or negative depending on

the state of switches S4 and S6. In order to exemplify the operation of the CFC, figure 2.24 shows the operation principle working with pair A.

The variables E, Ic , V_1 and V_2 are depicted considering constant line currents (I_{12} = 1.5 kA and I_{13} = 0.7 kA). From the previous analysis the voltage ripple can be deduced and it is given by equation (2.19).

$$\Delta E_{ripple} = \frac{I_{13} I_{12}}{fC(I_{12} + I_{13})} \tag{2.19}$$

where E_{ripple} is the voltage ripple of the capacitor, f is the switching frequency of the CFC and C is the CFC capacitance.

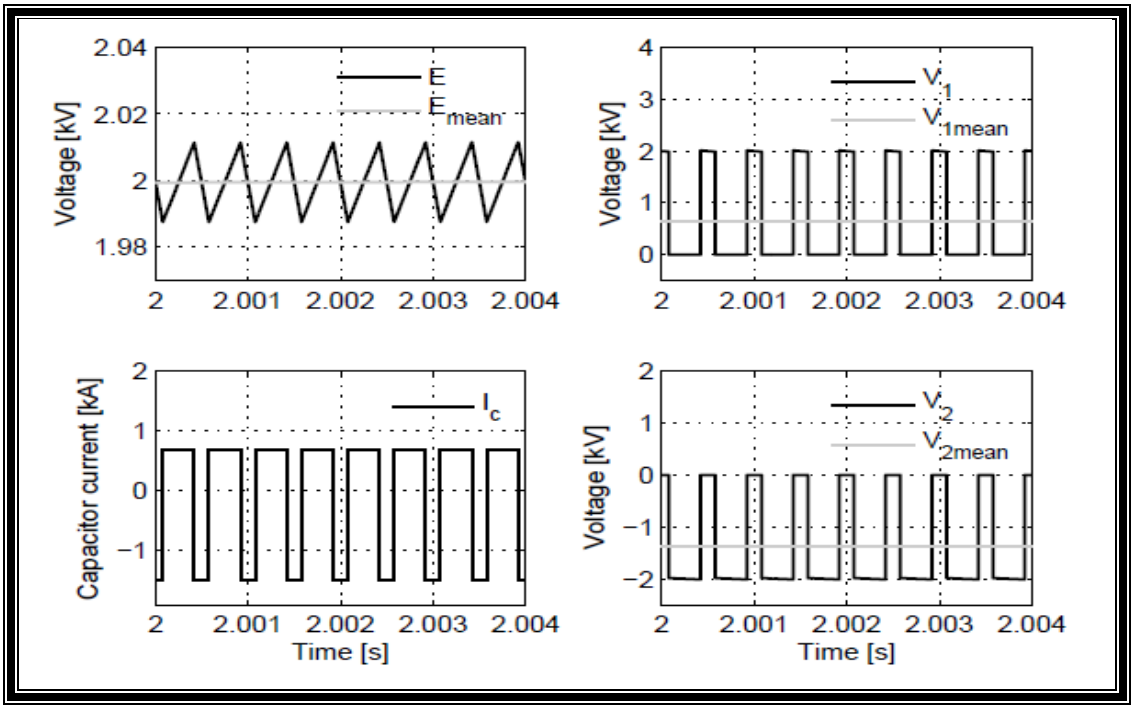

Fig.2.24. E, Ic , V_1 and V_2 working with pair A.

2.4.4 CFC average model

In this section an average model for the CFC is derived. The voltages applied by the converter considering pairs A, B, C and D are shown in table 2.1. Pairs A and B are applying opposite effects on the DC grid, the same happens with C and D. Whereas one increases I_{12}, the other rises the value of I_{13} .

Despite this fact, it is interesting to notice that voltages applied by the CFC have the same expression for both pairs (in both scenarios) with the difference of a sign. E must be always positive because of the inherent functionality of the device. When deriving an average model for the 4 pairs considered before, a restriction of positive value should be placed on variable E. Instead of restricting its value, it is chosen to allow negative values and using the equivalent model of pair A and D.

With this consideration, when solving the system equations, E will get a negative value when the opposite effect of pair A or D is expected. The negative value is not a real magnitude, it simply means that the CFC is working with pair B or C and the real average voltage of the capacitor is |E|.

Following this procedure, an equivalent model for the two current scenarios considered is derived. It includes two voltage sources in series with line cables. The values of these voltage sources V_1 and V_2 are

$$V_1 = (1 - D)\bar{E} \quad , \quad V_2 = -D\bar{E} \tag{2.20}$$

TABLE 2.1
CFC voltages applied for each pair of operation states

Pair	$\overline{V_1}$	$\overline{V_2}$
A	$(1 - D)\bar{E}$	$-D\bar{E}$
B	$-(1 - D)\bar{E}$	$D\bar{E}$
C	$-(1 - D)\bar{E}$	$D\bar{E}$
D	$(1 - D)\bar{E}$	$-D\bar{E}$

This model is illustrated in figure 2.25. This average model for two current flow configurations can be extended for all the possible current combinations (six possibilities) performing the same analysis as before.

A new duty cycle (line current relation) to represent each couple of voltage sources must be defined. The global average model for a CFC located in one node capable of operating with all current flow combinations can be made of three couples of voltage sources.

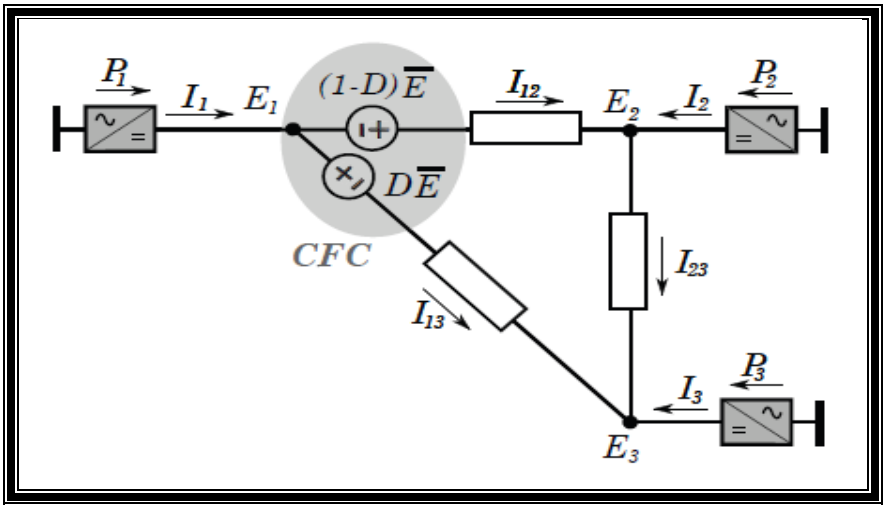

Fig.2.25: 3-terminal DC grid with a CFC average model in node 1

Chapter-III

A DC CFC for Meshed Modular Multilevel Converter Multi-terminal HVDC Grids

CHAPTER THREE

A DC CFC for Meshed Modular Multilevel Converter Multi-terminal HVDC Grids

3.1 Introduction

The HVDC transmission technology is recognized as an advantageous approach for worldwide long-distance bulk-power transmissions [13], with several HVDC applications currently in use for MTDC technologies [14]. Due to its superiority in more efficiently utilizing and integrating renewable energy located in remote areas, MTDC technology has become more attractive in recent years compared to traditional point-to-point HVDCs [15]. The MTDC system can also be reconfigured into different topologies under faults, particularly after a faulted line is isolated, in order to increase the continuity and reliability of the power supply [15]. Regarding the MTDC technology. Basically, the VSC based technology has more advantages over the LCC based technology [16]. This is because the vector control of the VSC converters, which realizes the independent control of active and reactive power. Hence, for the regulation of power, the VSC based MTDC system is considered more flexible, particularly in instances where the power flow reversal can be easily achieved by reversing the direction of DC currents rather than the reversal of DC voltages. Based on these characteristics, MTDC applications are being increasingly used in HVDC transmission.

Radial interconnections of DC grids, in particular, are being predominantly considered [17], due to their simple configuration and control strategies for regulating power distribution. In a radial topology, there is only one path between two electric nodes, so the power is fully regulated. Although the radial topology is simple and easy to realize, the meshed topology of DC grids, similar to that of AC grids, is considered as more favorable for real power applications [17]. This is because the meshed topology increases the redundancy of power transmission, which contributes to the enhancement of the reliability of the power system transmission [18].

In a meshed DC grid, the total power exchanged at the converter DC side can be fully controlled, however, the DC current of each branch, depending on the voltage difference of two DC

terminals and the resistance of the DC branch, may not be controllable. If there is no additional control strategy to balance the branch currents, the distribution of branch currents will be determined by Kirchhoff's laws.

There is a potential risk that one or more branches of a DC grid may become overloaded, while other branches may be underutilized, since more currents will inherently be delivered to the branch of lower resistance. Therefore, the complexity of the meshed DC grid leads to the potential problems, which are the main concerns of this chapter.

There are several control strategies for meshed MTDC grids that have been proposed in the literature. Different droop controllers have been investigated for MTDC grids including meshed topologies. It was found that while the active power of each terminal could be coordinated to a certain extent, the distribution of the DC current on each branch was incapable of being accurately controlled in the meshed grid. A power flow control device for a meshed DC grid has been designed and demonstrated in [17]. In this work, the DC branch current is well controlled by switching on and off the variable resistance of the device. However, the power loss due to switch-in resistance is an undesirable outcome. Reference [19] has presented a power flow control device that provides a detailed system configuration and basic control logic for a meshed DC. However, the control strategy in this device has not been comprehensively analyzed nor a detailed control strategy proposed. A conceptual DC control flow controller (CFC) has been proposed in which standard full-bridge DC-DC converters with low voltage ratings are used to design the controller. However, only a basic conceptualization of this control device is introduced, and the performance of the branch current control capability is not fully illustrated, while the operating principle and detailed control approach of the device are also not thoroughly investigated.

In this chapter, the design of a DC CFC, particularly its detailed control strategy of branch currents, is proposed for a meshed 3-T MMC HVDC grid. The objective of the DC CFC is to control the DC branch currents by transferring the additional power from the overloaded branch to the underutilized branch and to realize this objective with relatively low power losses. The DC branch currents can be regulated at a certain range using the proposed control. The validity of the proposed control strategy of the DC CFC is verified through case studies on the RTDS. The rest

of this chapter is organized as follows. Section 3.2 presents the meshed 3-T MMC-HVDC system with the system configuration, the control strategy of the MMC at each terminal and an equivalent DC power flow analysis. Section 3.3 introduces the meshed MTDC system with the installation of a DC CFC along with the structure of the DC CFC. Section 3.4 explains the proposed control strategy of the DC CFC and features with the proposed control.

3.2 Meshed 3-T Modular multilevel converter MMC-HVDC System

3.2.1 System Configuration

A single-line schematic diagram of the investigated meshed 3-T MMC-HVDC system is shown in figure 3.l(a). The three terminals are T1, T2, and T3. The MTDC system has three (3) identical Modular Multilevel Converter (MMCs). Each MMC, as shown in figure l(b), comprises six (6) converter arms and each arm has n series half-bridge Sub-module (SMs) and one series inductor L_{arm} per converter arm. Each SM includes an energy storage capacitor (C) and two switching valves (S_1, S_2). Only one switch is switched on during normal operation. Therefore, the output voltage V_{SM} of each SM is either equal to the capacitor voltage V_C when the upper switch S_1 is switched on, or equal to zero when the lower switch S_2 is switched on. The MMC modeled in this thesis has 6 SMs per converter arm. The MMC DC side is connected to the DC cable, while the MMC AC side is connected to an AC grid at each terminal through a series inductor and resistor as well as a three-phase transformer.

3.2.2 Control Strategies of the MMCs

The MMCs are considered as VSC type converters [20],[21]. The converter level control of the model in this chapter applies the classic vector control strategy. Both MMC1 and MMC2 apply constant active power control. For the sake of simplification of the system analysis, some assumptions are made:

- The losses of the converters are neglected.
- The AC system voltage is constant due to the connection to the AC utility grid.
- The MMC DC side current is regulated to be constant via the active power control.

The total current imported from T_1 to the DC grid is kept at 1 kA, while the total current exported from the DC grid to T_2 is kept at 0.4 kA. MMC3 is controlled to maintain the DC voltage of T_3 at ±50 KV. The reactive power is controlled to be at 0 by all three MMCs.

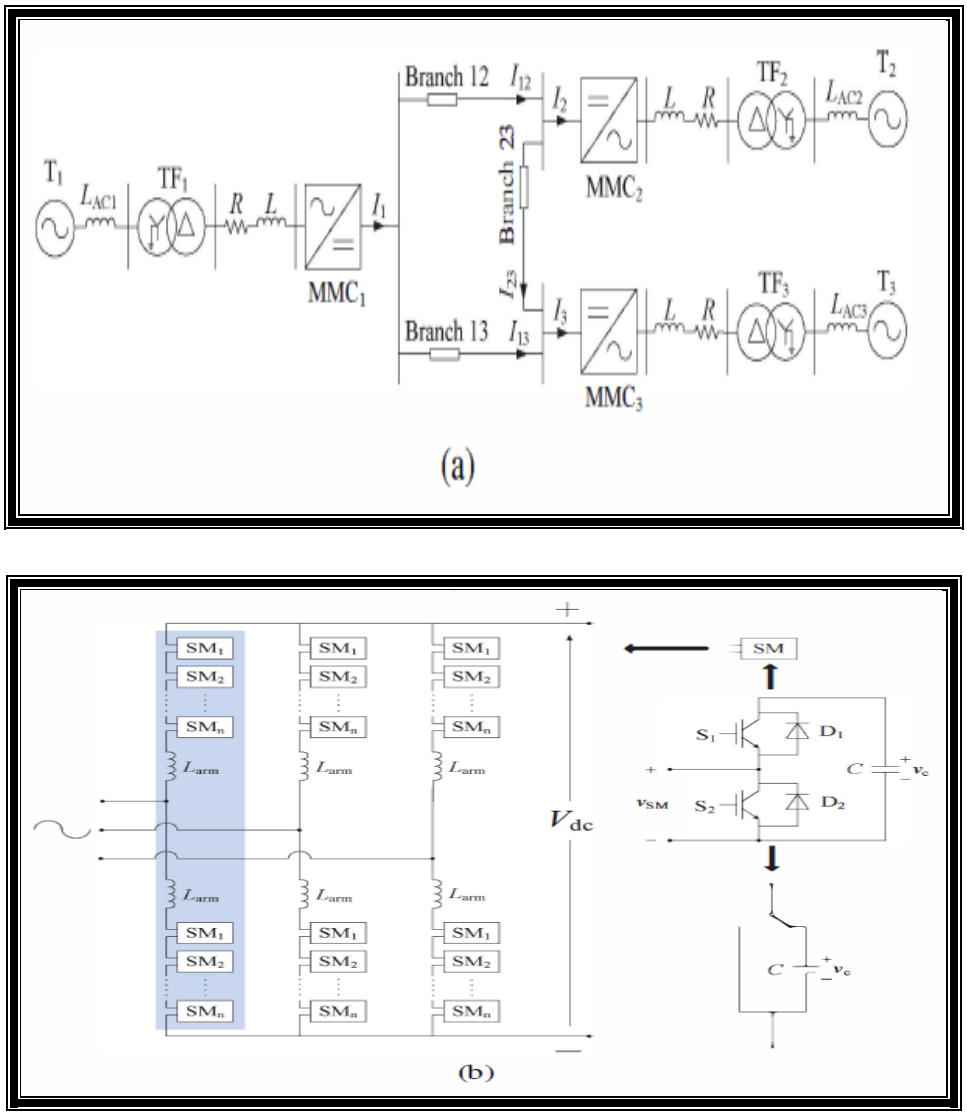

Fig. 3.1. Configuration of a meshed 3-T MMC-HVDC grid.

(a) System configuration. (b) MMC configuration.

The capacitor voltage balancing strategy of the MMC employs the conventional sorting method [16]. That is, depending on the arm current direction, the capacitor with a relative lower voltage is charged first, while the capacitor with a relative higher voltage also discharges first.

The DC branch currents I_{12}, I_{13} and I_{23}, which flow via Branch 12, 13, and 23, are not controlled. Thus the distribution of the branch currents largely depends on the cable resistance of each branch. Although most DC cables are constructed of the same material, the lengths of the DC cables between terminals are different and environmental conditions, such as temperature may lead to differences in cable resistance. Therefore, in principle, the cable resistance of each branch is considered to have different values.

If there is no additional strategy to control the DC branch current, the distribution of branch currents, for instance, I_{12}, I_{13} and I_{23}, of the DC grid, are uncontrollable. One or more branches, therefore, may become overloaded, while the other is insufficiently utilized. The principle of electric power transmission is to achieve a maximum utilization of the transmission line/cable within its transfer capability [15]. Therefore, the control of the branch currents is inevitable and necessitates additional controllers.

The branch currents of a meshed DC grid are determined by DC cable resistances and DC voltage differences between two terminals, two approaches can be used to control the branch current.

- One is to change the cable resistance by adding an additional resistor on the DC branch. this method significantly increases power losses, which are undesirable.
- The second method aims at changing the voltage difference between two DC terminals to regulate the branch current. This method is considered a preferable approach since the branch current control is achieved with acceptable low power losses.

3.2.3. Equivalent Power Flow Analysis of the Meshed MTDC

Grid The DC nominal voltage of T_3 is regulated at ±50 kV, via the control of MMC3. Hence, the DC voltage of T_3, V_3, is 100 KV. T_1 imports 1 kA to the DC grid, while T_2 exports 0.4 kA from the DC grid. Thus, the DC currents I_1 and I_2 are 1 kA and 0.4 kA, respectively. The DC buses of MMCI and MMC2 can be simplified and regarded as two ideal DC current sources, while the DC bus of MMC3 can be considered as an ideal voltage source. The diagram in figure 3.2 presents the simplifications of the DC grid. An equivalent power flow analysis is conducted based on figure 3.2.

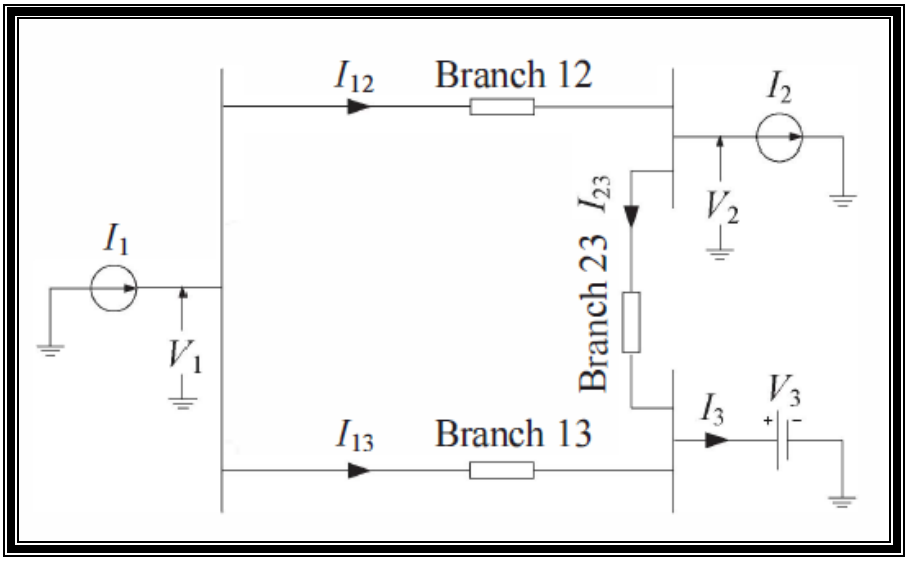

Fig.3.2 Configuration of the 3-T MMC-HVDC grid.

Based on Kirchhoff Current Law (KCL), the currents in the meshed MTDC grid have the following relationships:

$$I_1 = I_{12} + I_{13} \tag{3.1}$$

$$I_3 = I_{23} + I_{13} \tag{3.2}$$

$$I_1 = I_2 + I_3 \tag{3.3}$$

According to Ohm's Law, the branch currents in figure 3.2 can be derived as:

$$I_{12} = \frac{V_1 - V_2}{R_{12}} \tag{3.4}$$

$$I_{13} = \frac{V_1 - V_3}{R_{13}} \tag{3.5}$$

$$I_{23} = \frac{V_2 - V_3}{R_{23}} \tag{3.6}$$

The values of I_1, I_2, and V_3 are determined by the control of MMCs, which means there are six unknown variables in (3.1)-(3.6). Therefore, all of their values can be obtained. The expressions of V_1, I_3 and V_3 are derived in (7)-(9).

$$v_1 = v_3 + \frac{I_1 R_{13}(R_{12} + R_{23)} - I_2 R_{23} R_{13}}{R_1 + R_2 + R_3} \tag{3.7}$$

$$I_3 = I_1 - I_2 \tag{3.8}$$

$$v_2 = v_3 + \frac{I_1 R_{23} R_{13} - I_2 R_{23}(R_{12} + R_{13})}{R_1 + R_2 + R_3} \tag{3.9}$$

Referring to the cable parameters listed in appendix (A) and the output DC currents and voltage of the MMCs where I_1 = 1 kA, I_2 = 0.4 kA, V_3 = 100 kV, the voltages and currents of the DC grid are:

DC terminal voltages: V_1 = 100.8 kV, V_2 = 100.2 kV, V_3 = 100 kV.

DC terminal currents: I_1 = 1 kA, I_2 = 0.4 kA, I_3 = 0.6 kA.

DC branch currents: I_{12} = 0.6 kA, I_{13} = 0.4 kA, I_{23} = 0.2 kA.

From the power flow analysis, it is observed that the branch current I_{12} is larger than I_{13}. However, the cables in both branches are made from the same material and thus have the same transfer capability. Hence, Branch 12 is either overloaded or getting closer to its transfer limit, while Branch 13 is insufficiently utilized. Under this condition, a DC CFC with the capability of balancing the branch currents is needed for the meshed MTDC grid to deal with the aforementioned problem, which is discussed in the following sections.

3.3 DC CURRENT FLOW CONTROLLER (DC CFC):

3.3.1 Meshed MTDC System with a DC CFC

The DC CFC is equipped on Branch 12 and Branch 13. Fig. 3.3 shows a single-line schematic diagram of the developed meshed 3-T MMC-HVDC system with the DC CFC being equipped.

The expected operating condition of the power transmission system is to keep each branch working at its optimal transfer capacity, and this is achievable by the control of the DC CFC, which will be explained in Section 3.4.

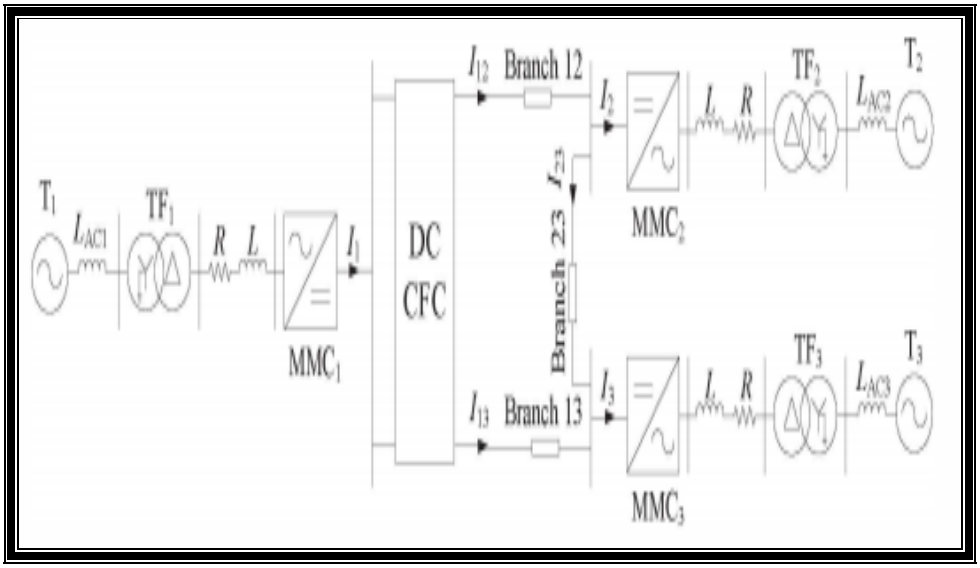

Fig. 3. 3-T MMC-HVDC system with the installation of the DC CFC

3.3.2 Structure of the DC CFC

The detailed structure of the DC CFC installed between Branch 12 and Branch 13 is shown in figure 3.4. The DC CFC is composed of two identical full-bridge DCDC converters. figure 3.5 shows the diagram of an independent full bridge DC-DC converter. A DC-DC converter has two legs and one energy storage capacitor in the middle. Each leg comprises two IGBTs with their anti-parallel diodes.

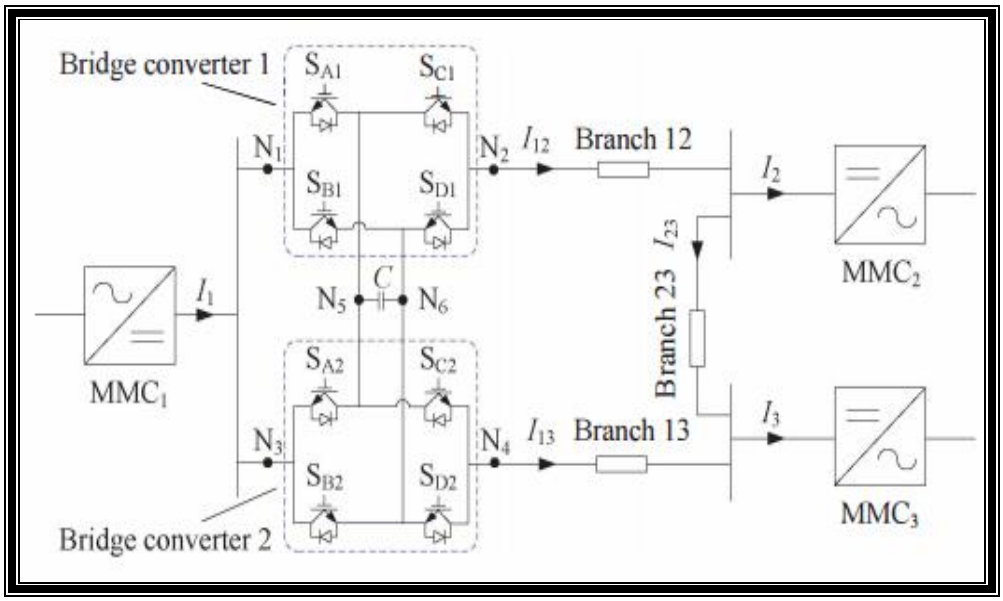

Fig. 3.4. Structure of the DC CFC

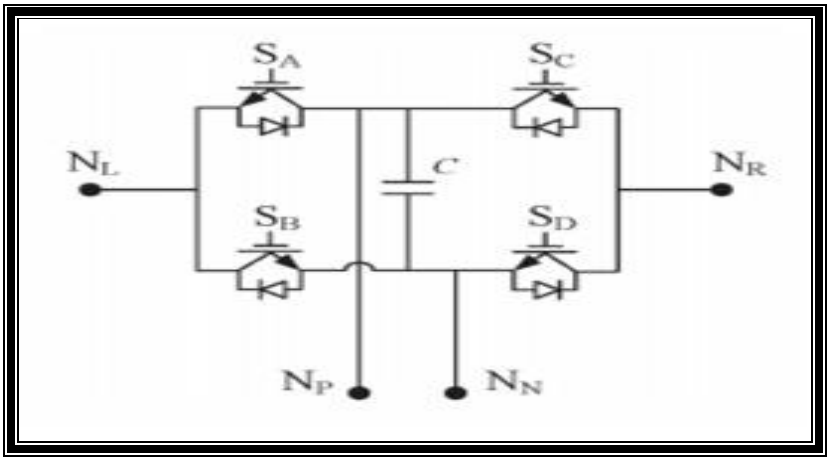

Fig. 3.5. Full bridge DC-DC converter

S_A and S_B are on the same leg, while the other two (S_C and S_D) compose the other leg. Two switches on the same leg are switched complementary. Consequently, when S_A is in its off state, S_B is in the on state, which is the same for S_C and S_D. This operation manner ensures the two switches on the same leg are never of simultaneously. Under this switching specification, the current through the capacitor is always continuous. The capacitor has three operational states with different switching modes, bypassed, charged, and discharged, as shown in Table 3.1. The capacitor is bypassed when both S_A and S_C are on or both S_B and S_D are on. The capacitor is charged when both S_A and S_D are on, while the capacitor is discharged, when both S_B and S_C are on. The DC CFC is composed of the connection of two DC-DC converters. The interconnection points are the positive and negative side (N_P, N_N) of the capacitor, respectively, as shown in figure 3.5

TABLE 3.1

SEITCHING MODES WITH CAPACITOR STATUS

Mode	Capacitor State	S_A	S_B	S_C	S_D
1	Bypassed	ON	OFF	ON	OFF
2	Bypassed	OFF	ON	OFF	ON
3	Charged	ON	OFF	OFF	ON
4	Discharged	OFF	ON	ON	OFF

3.4 CONTROL STRATEGY OF THE DC CFC

The objective of using the DC CFC is to realize the control of the branch currents in the meshed 3-T MMC-HVDC grid. The equivalent power flow analysis of the meshed MTDC grid derived in Section 3.2.3 indicates that it is necessary to balance the current distribution of Branch 12 and Branch 13 through the control of the DC CFC. This is achieved by transferring additional power from Branch 12 to Branch 13 via the energy storage capacitor.

Under steady-state condition, the imported and exported power of the interconnected capacitor should be equal. In order to realize the control of the branch currents, not only the branch current I_{12} needs to be regulated, but the voltage of the interconnected capacitor V_C needs to be controlled as well. This is because a stable capacitor voltage indicates that the power exchange of the capacitor is balanced. In addition, the voltage of a capacitor represents the energy stored in the capacitor. The energy of a capacitor can be approximately represented by its average voltage:

$$w_C = \frac{1}{2} C V_c^2 \tag{3.10}$$

V_C is the average voltage stored in the capacitor. The power imported and exported of a capacitor is depicted in figure 3.6.

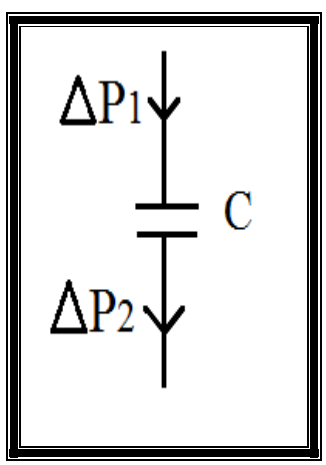

Fig. 3.6. Power imported and exported of a capacitor.

Under steady-state conditions, the power exchange of the interconnected capacitor is balanced, so

$$\Delta P_1 = \Delta P_2 \tag{3.11}$$

That means the power imported to the capacitor equals to the power exported from the capacitor, so the power of the capacitor $\mathrm{P_c}$ is zero. As power is defined as the derivative of work, we have

$$\frac{\mathrm{dW_c}}{\mathrm{dt}} = \mathrm{P_c} = 0 \tag{3.12}$$

According to (3.10) and (3.12), the capacitor voltage should be controlled to maintain a certain value under steady-state conditions based on the operating condition of the DC CFC. The basic control strategy of the DC CFC is similar to that of a point-to-point VSC-HVDC system in which DC voltage control is employed by one converter station at one terminal to maintain the voltage of the DC grid, while active power flow control is applied by the other converter station to determine the amount of power and its direction. Therefore, one terminal is operated as a slack DC terminal, the active power of which can be either imported or exported depending on the operating condition of the other terminal.

For the DC CFC modeled in this chapter, the DC-DC converter on Branch 12 is assigned to control branch current I_{12}. When I_{12} is controlled, the current on Branch 13, I_{13}, is determined simultaneously. This is because the total current of Branch 12 and Branch 13, I_1 is regulated at 1K by the control of MMC1. The other DC-DC converter on Branch 13 is responsible for regulating the voltage of capacitor C_2. Since two capacitors of the DC-DC converters are connected in parallel, they always have the same voltage value.

From the structure of the DC CFC, as shown in figure 3.4, S_{A1} and S_{A2} are connected in parallel, and this is same for S_{B1} and S_{B2}. Thus, to maintain the voltage of the capacitors, the operation of S_{A1} and S_{A2} must be synchronous. Meanwhile, the operation of S_{B1} and S_{B2} are also synchronous and should be complementary with S_{A1} and S_{A2}. In fact, in the existence of S_{A1} and S_{B1} of the DC-DC converter on Branch 12, S_{A2} and S_{B2} of the other DC-DC converter are not necessarily needed. However, in order to maintain a higher redundancy of the meshed DC grid, four switches on both DC-DC converters are retained. In addition, S_{A1} and S_{A2} are both named as

S_A with a same controlled gating signal (G_A) while S_{B1} and S_{B2} are both named as S_B with a complementary gating signal (G_B) [22].

According to Table 3.1, the capacitor of the DC-DC converter shown in figure 3.5 is charged with switching mode 3 and is discharged with mode 4. The duty ratio of each switch of the full-bridge DC-DC converter is D_{SJ} (J = A, B, C, D) and the generated gating signal is G_{SJ}. The gating signal is produced through the PWM by comparing the controlled signal with a saw tooth wave. Two general operating states within two switching cycles are depicted in figure 3.7.

In figure 3.4, Branch 12 needs to transfer its power to Branch 13 by charging the interconnected capacitor, while Branch 13 needs to obtain the excess power from Branch 12 by discharging the interconnected capacitor. Due to the characteristics of complementary switching, only one switch on one leg needs to be controlled. For the DC CFC modeled in this chapter, S_A, S_{C1} and S_{C2} are controlled. In order to simplify the following analysis, the duty ratios of S_A and S_B, D_{SA} and D_{SB} are both fixed at 0.5. The branch current control and the capacitor voltage control will thus be achieved by controlling the switches S_{C1} and S_{C2}.

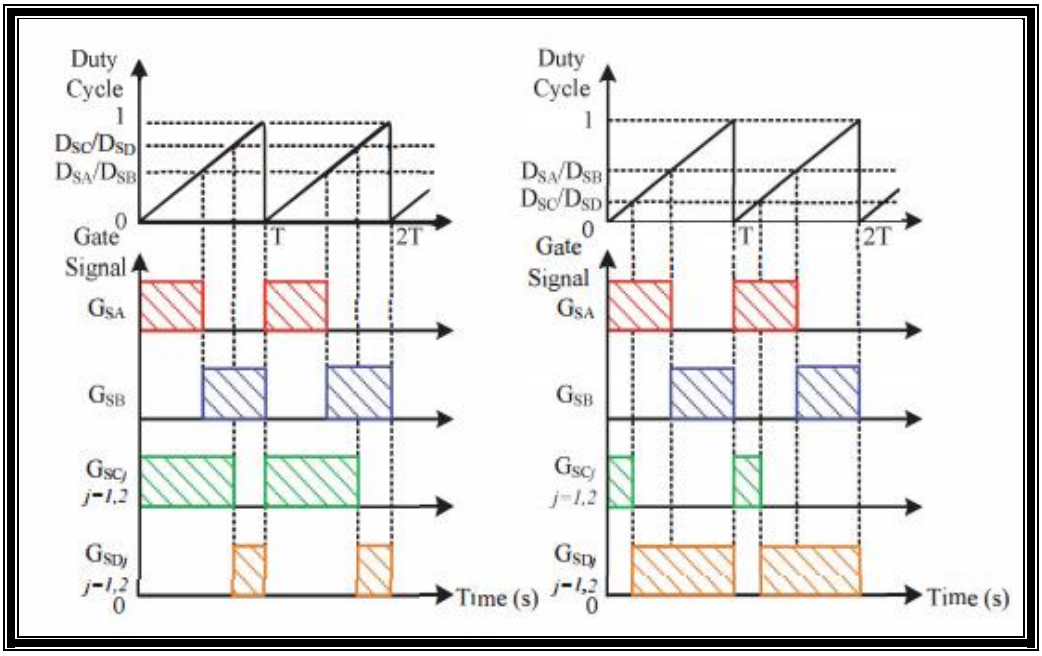

Fig. 3.7, Gate signal generation of each switch

3.4.1 Branch Current Control

The branch current control is implemented through regulating the difference of the duty ratio between S_A and S_{C1}. As the switching performance is shown in figure 3.7, when the duty ratio difference D_{SA} - D_{SC1} is positive, the interconnected capacitor is charged and I_{12} becomes smaller. The measurement of branch current 12 (I_{12meas}) is tracking its reference value (I_{12ref}) by the application of a **PI** controller. Figure 3.8 illustrates the control approach. In figure 3.8, a larger (smaller) I_{12meas} than I_{12ref} leads to a decrease (increase) in the generated duty cycle of S_{C1}. Thus, the interconnected capacitor will be charged (discharged) more with switching mode 3 and I_{12meas} will be reduced (increased) to track I_{12ref}.

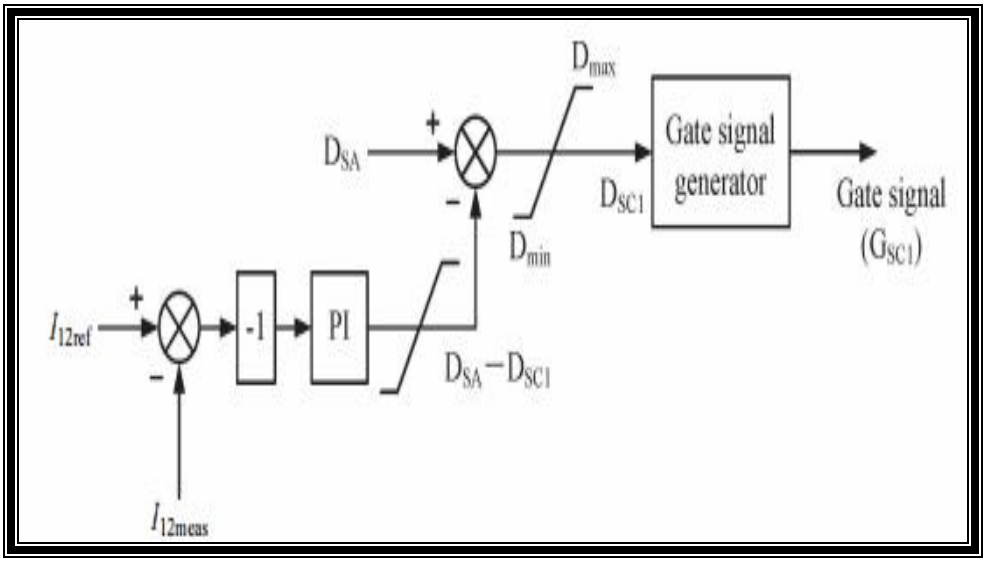

Fig. 3.8, Branch current control system.

3.4.2 Capacitor Voltage Control

The control of the capacitor voltage is similar to that of the branch current, via a **PI** controller. The control approach is illustrated in figure 3.9. A positive (negative) tracking error signifies the measured capacitor voltage is smaller (larger) than its reference voltage and will result in a decrease (increase) in the generated duty ratio of S_{C2}. Thus, the interconnected capacitor will be charged (discharged) with switching mode 3 and V_{Cmeas} will be increased (decreased) to track the control reference.

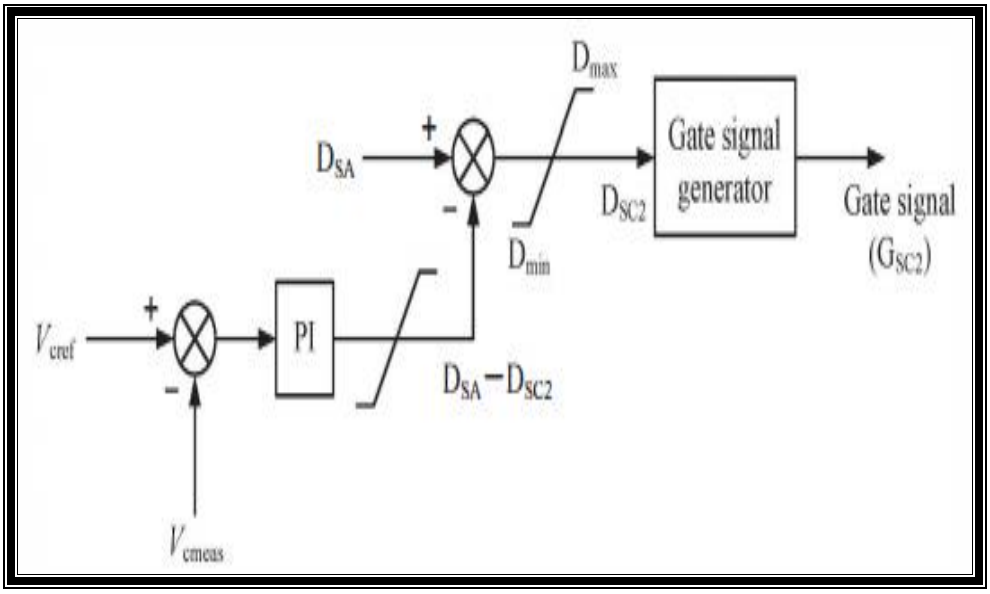

Fig. 3.9. Capacitor voltage control

3.4.3 Start-up Process of the DC CFC

Initially, the DC CFC is in standby mode, i.e., the interconnected capacitor is bypassed, so the capacitor voltage is zero and the branch currents are not controlled. I_{meas} (0.6 kA) is larger than the reference value (0.5 kA).

When the DC CFC is started to control the branch currents, the duty ratios of S_{C1} and S_{C2} generated are both decreased, leading to the charging of the interconnected capacitor. Hence, the voltage of the interconnected capacitor will be fast charged to the reference value and I_{meas} will decrease during the charging process.

A new steady-state condition will be achieved when the power exchanged between the capacitor is balanced, the voltage of the capacitor is well maintained and the branch current is regulated to the reference value.

3.4.4 Features of the DC CFC

The DC CFC with the proposed control has two main features: I-branch current balancing capability; II- branch current regulating capability.

I. Branch Current Balancing Capability:

In the meshed MTDC grid, an equal distribution of the branch currents at one terminal junction is expected when the transmission capabilities of both cables are the same. Different lengths of branches and the impact of the environmental conditions lead to different cable resistance, so the natural distribution of branch currents in a meshed grid is usually unbalanced. The DC CFC with the proposed control in the meshed MTDC grid has the ability to regulate the DC branch current to achieve equal distribution of the branch currents.

II. Branch Current Regulating Capability:

In some meshed MTDC applications, the transmission capabilities of DC cables are different, it is expected that the power transfer on one branch can be operated over another branch. Hence, instead of the equal DC branch current distribution, a proportional distribution of the branch currents at one terminal junction is desired to facilitate the optimal operating state of each branch. The DC CFC with the proposed control is capable of regulating the DC branch currents within a certain range.

Chapter-IV

Results and Discussion

CHAPTER FOUR

RESULTS AND DISCUSSION

4.1 Simulation Systems

The simulation system is the meshed 3-T MMC-HVDC system, as shown in chapter three figure 3.3, using the parameters provided in appendix A. The structure of the DC CFC used in the simulation as shown in figure 4.1. The interconnect capacitor C is 30 μF, and the rated voltage of the IGBTs of the DC CFC is 10 kV.

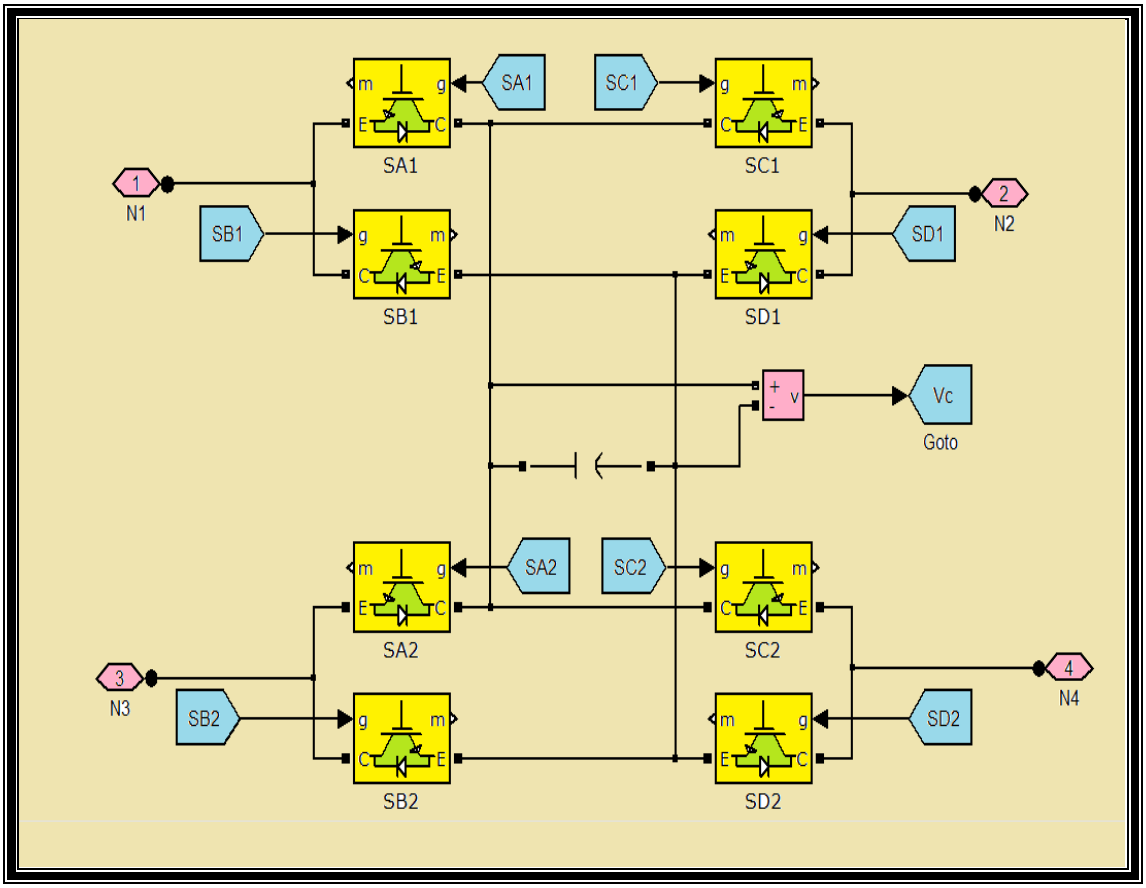

Fig 4.1 Simulation of the DC CFC

4.2 Case Studies

4.2.1 Branch Current Balancing Capability

Initially, the DC CFC is in standby mode. The DC CFC starts to balance the branch currents at 1 sec. I_{12ref} is set to 0.5 kA, and V_{Cref} is set to 1 kV.

Figures 4.2 - 4.5 shows System performance with branch current balancing control of the DC CFC.

- Figure 4.2 shows the MMC DC side current at each terminal. I_1 = 1 kA, I_2 = 0.4 kA, and I_3= 0.6 kA. Only a small ripple is observed at 1 sec when the DC CFC is operating to balance the branch currents.
- Figure 4.3 shows three branch currents with natural distributions of each terminal before 1 sec. It is observed that by bypassing the interconnected capacitor at the initial stage, the DC CFC does not perform the balancing function of the branch currents and the system is operating just as the system shown in figure 3.l(a) in chapter three without the DC CFC in which branch current I_{12} = 0.6 kA, I_{13} = 0.4 kA, and I_{23} = 0.2 kA at 1 sec., both I_{12} and I_{13} reach 0.5 kA within 0.5 sec.
- The DC voltage of the interconnected capacitor is shown in figure 4.4. The capacitor voltage V_C is zero when the capacitor is bypassed. At 1 sec, the power is transferred via the capacitor, and V_C is charged to 1 kV within 0.1 sec.
- The DC side voltage of MMC3 is shown in figure 4.5. V_3 has a small voltage drop when the balancing control of the branch current is applied, but it resumes 100 kV within 1 sec. The overall results indicate the effectiveness of the DC CFC in balancing the branch currents.

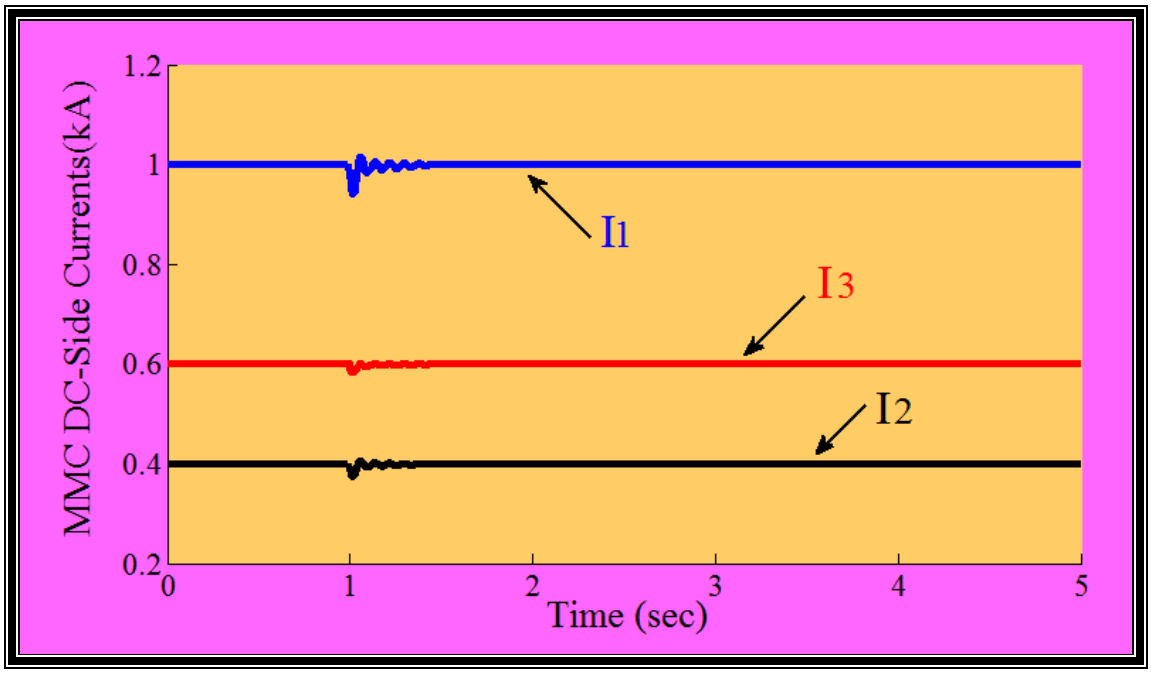

Fig 4.2 MMC DC-Currents , I_1, I_2, I_3 are the DC currents of T_1, T_2, and T_3, respectively

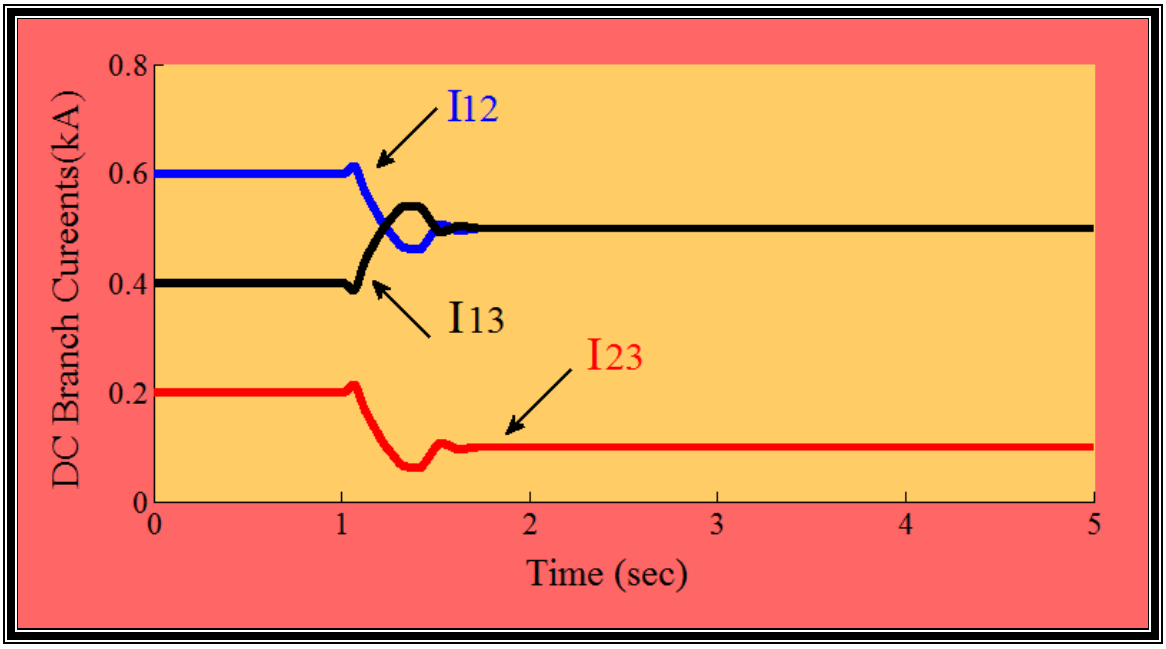

Fig 4.3 DC Branch Current I_{12}, I_{13}, and I_{23} are the DC currents of Branch 12, 13, and 23, respectively

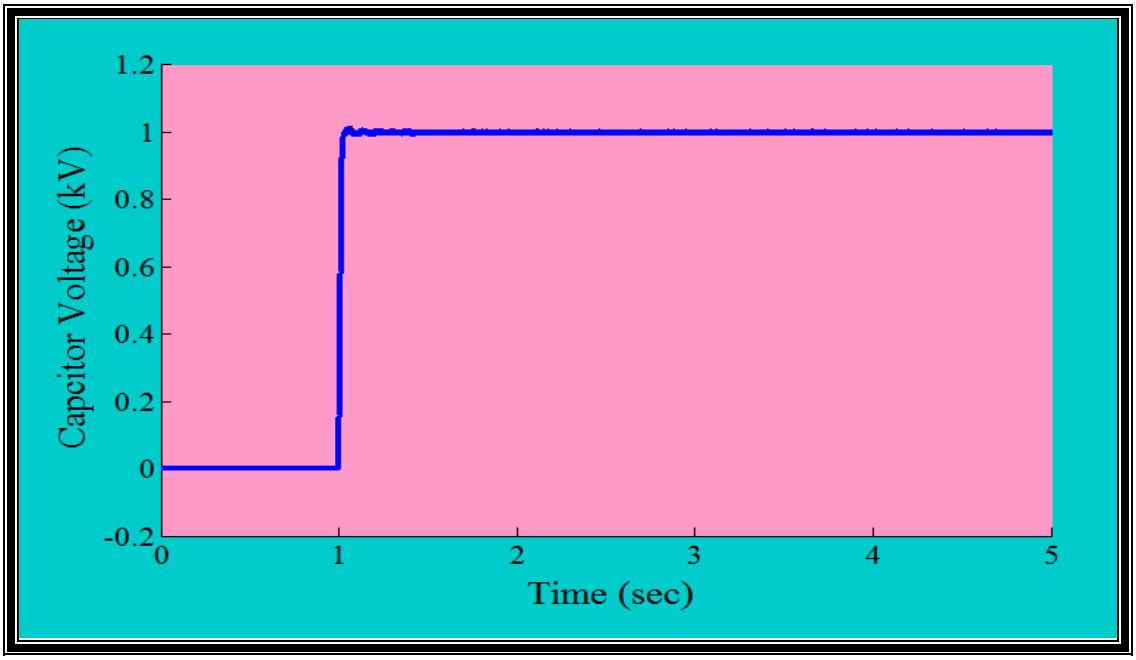

Fig 4.4 Voltage of the interconnected capacitor

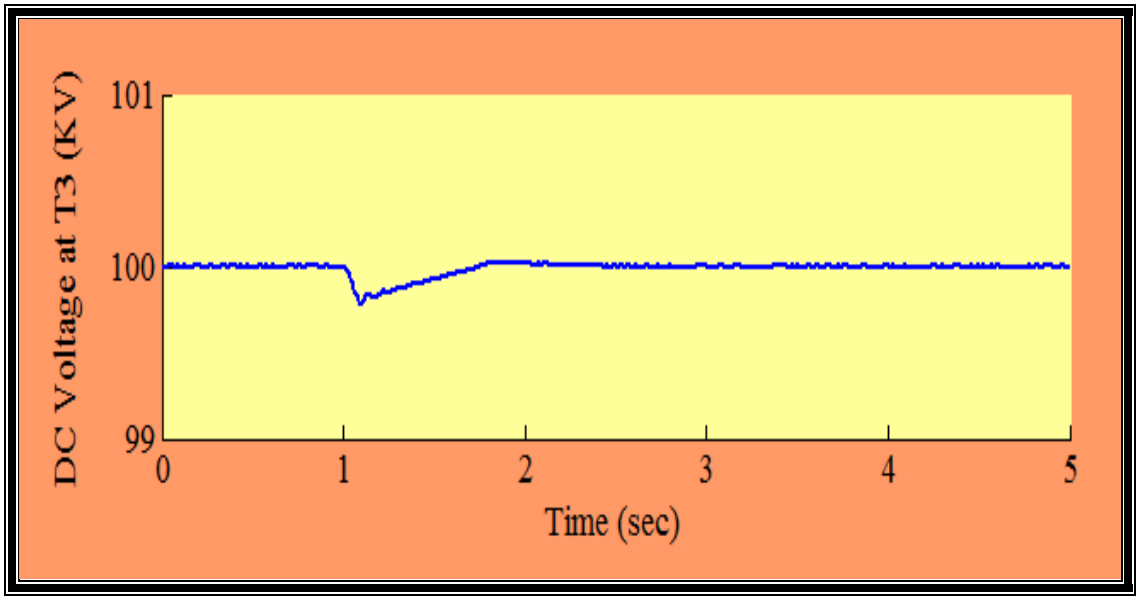

Fig 4.5 DC voltage at T3

4.2.2 Branch Current Regulating Capability

Initially, the DC CFC is with the mode of balancing the branch current. At Is, the logic of regulating the branch currents performs its role where I_{12ref} is set to 0.7 kA, and V_{Cref} is still set to 1 kV.

Figures 4.6 - 4.9 show System performance with branch current regulating control of the DC CFC.

- Figure 4.6 demonstrates that the currents at three DC terminals are well stabilized at their reference values after applying the branch current regulating control of the DC CFC.
- Figure 4.7 shows that at 1 sec, I_{12} is tracking its reference signal to 0.7 kA, while I_{13} is decreasing to 0.3 kA and I_{23} is increasing to 0.3 kA; both branch currents reach the new steady-state condition within 1 sec.
- The voltage of the interconnected capacitor is maintained at 1 kV with a small voltage dip as shown in figure 4.8.
- The DC voltage of T3 and V_3, has a slight decrease after 1 sec, but it returns to the reference voltage within 1 sec, as shown in figure 4.9.

The performance of the branch currents and capacitor voltage validate the branch current regulating control of the DC CFC.

The simulation results shown in figures 4.2 - 4.9 illustrate that the branch currents can not only be equally distributed, but also be regulated within a certain range as well.

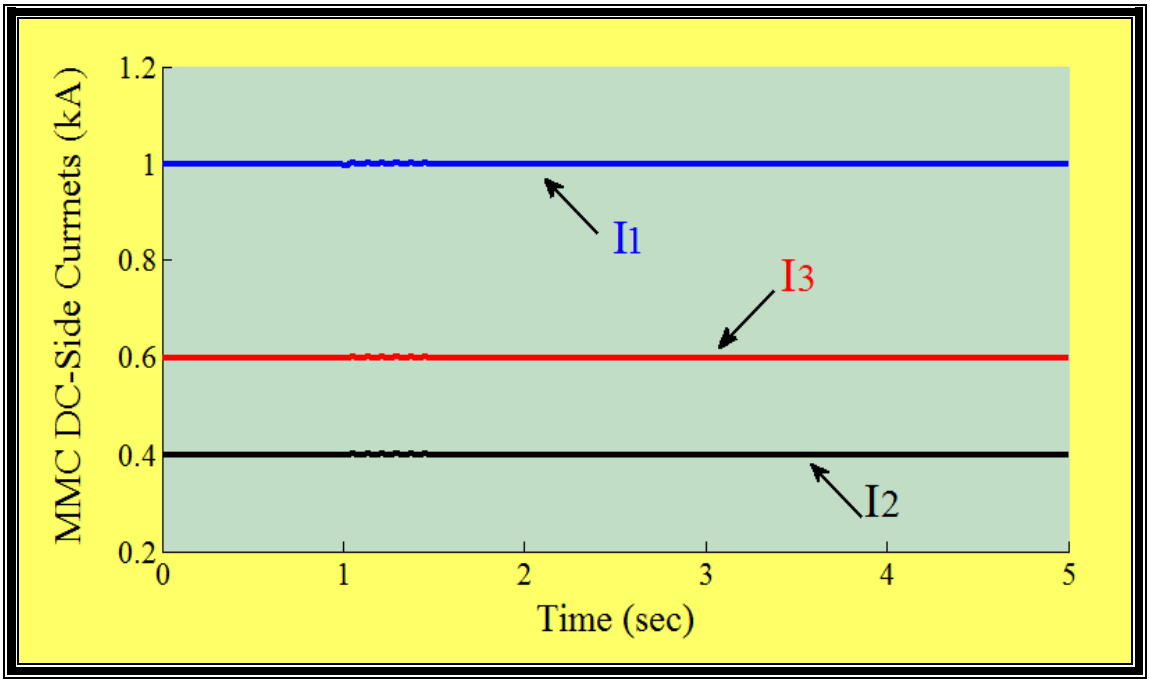

Fig 4.6 MMC DC-Currents , I_1, I_2, I_3 are the DC currents of T_1, T_2, and T_3, respectively

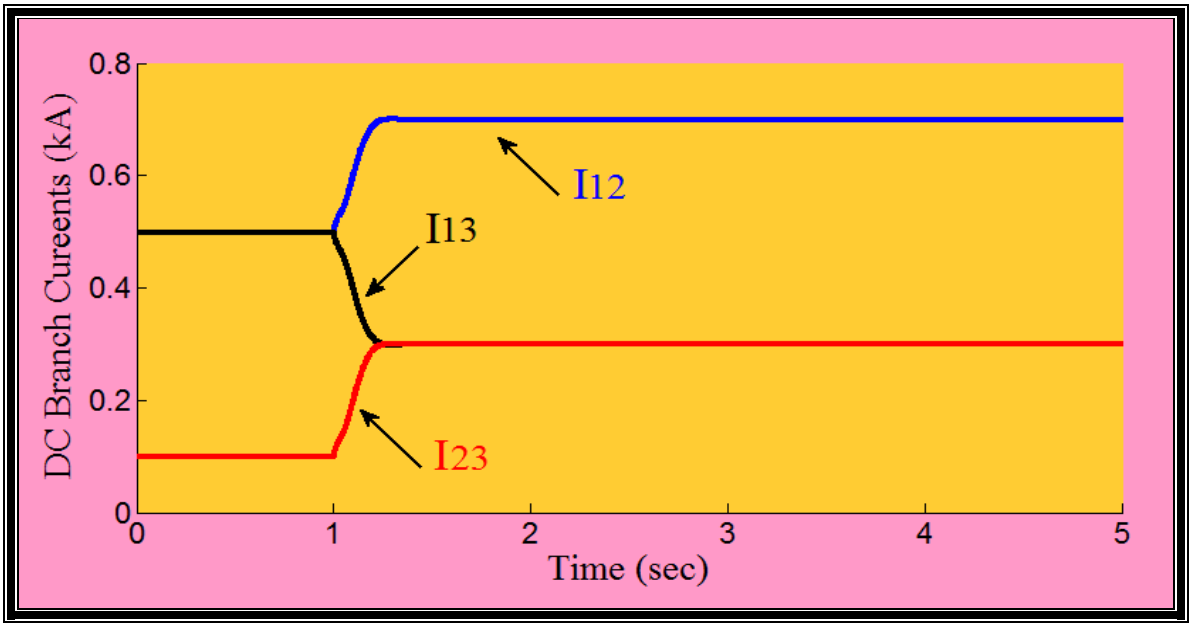

Fig 4.7 DC Branch Current I_{12}, I_{13}, and I_{23} are the DC currents of Branches 12, 13, and 23, respectively

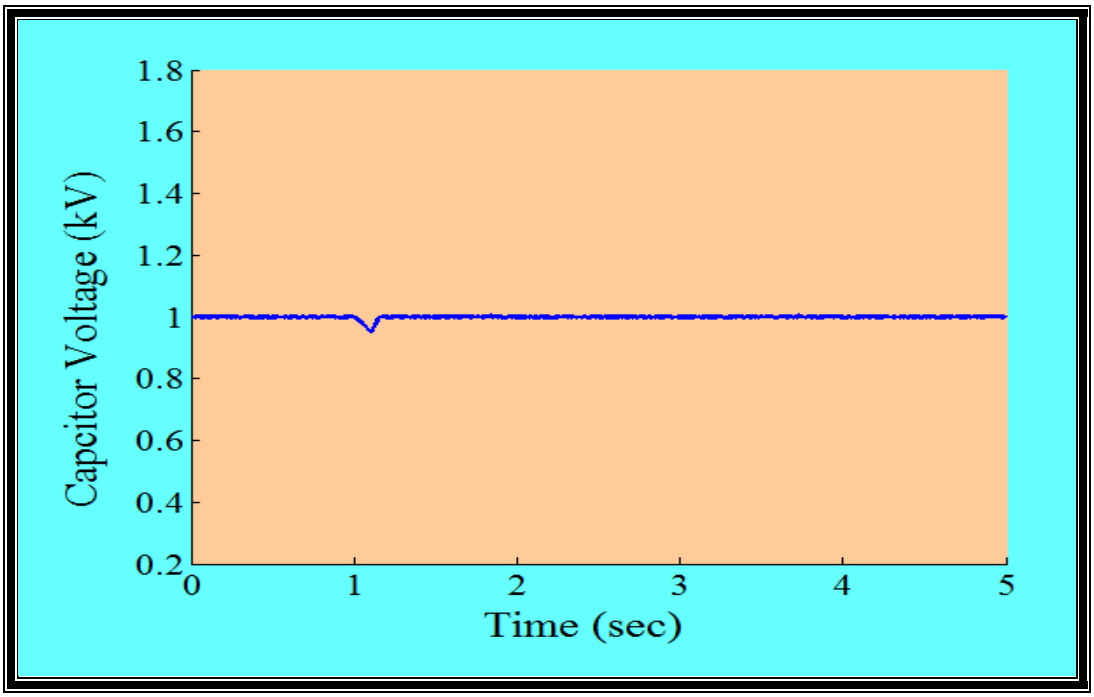

Fig 4.8 Voltage of the interconnected capacitor

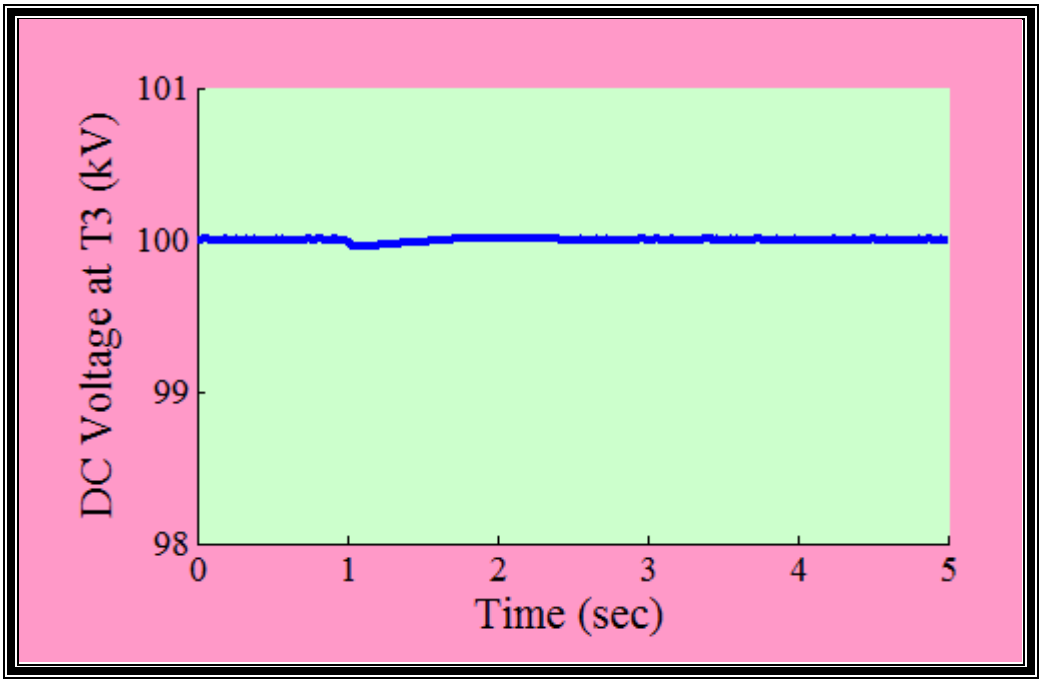

Fig 4.9 DC voltage at T3

Chapter-V

Conclusion and Suggestions for Future Work

CHAPTER FIVE

CONCLUSION AND SUGGESTIONS FOR FUTURE WORK

5.1 Conclusion

- In this thesis has proposed the design of a DC CFC, particularly its detailed control strategy, in order to control the branch currents in a meshed 3-T MMC-HVDC grid.
- An equivalent power flow analysis of the 3-T meshed grid under the steady-state condition has been derived. It has been found that for the system without DC CFC, the branch currents are uncontrollable and one or more branches may become either overloaded or underutilized.
- The structure of the DC CFC has been presented with its operation theorem being proposed.
- The DC CFC has features of branch current balancing and regulating capability with the proposed control, which has been validated through case studies on the RTDS. These features allow the branches to avoid overloading and to operate under optimal condition.
- This DC CFC with the proposed control can be regarded as an effective model for the branch current control in a meshed DC grid.

5.2 Suggestions for future work

- Having gone through the study of DC CFC for a meshed 3-T MMC-HVDC grid.
- We can general work for up a meshed 3-T MMC-HVDC grid and study power flow in network.
- Also we can used the fuzzy logic replace PI control to get more good results for power flow grid to improve the DC power flow grid.

REFERENCE

[1] HVDC Applications and Beni_t History, Siemens website. http://www.energy. siemens.com/co/en/power-transmission/hvdc/applications-benefits/ hvdc-history.htm. Accessed: 2015-06-14.

[2] E. W. Kimbark. Direct Current Transmission. Wiley, New York, vol. 1 edition, 1971.

[3] HVDC Light, its time to connect, ABB website. //http://new.abb.com/docs/ default-source/ewea-doc/hvdc-light.pdf?sfvrsn=2. Accessed: 2015-06-14.

[4] HVDC for beginners and beyond, ALSTOM website. //http://www.alstom.com/ Global/Grid/Resources/Documents/Systems/HDVC%20for%20beginners%20and% 20beyond%20Brochure%20GB.pdf. Accessed: 2015-06-14.

[5] D. R. Trainer C. D. Barker, C. C. Davidson and R. S. Whitehouse. Requirements of DC-DC Converter to facilitate large DC grids. In CIGRE Session 2012, 2012.

[6] Jiebei Zhu and C. Booth. Future multi-terminal HVDC transmission systems using Voltage source converters. In Universities Power Engineering Conference (UPEC), 2010 45th International, pages 1{6, Aug 2010.

[7] Mu Q, Liang J, Li Y L, et al.Power flow control devices in DC grids[C]//2012 IEEE Power and Energy Society General Meeting.San Diego, CA: IEEE, 2012:1-7.

[8] Wen Jialiang, Wu Rui, Peng Chang,et al.Analysis of DC grid prospects in China[J].Proceedings of the CSEE,2012,32(13):7-12(in Chinese).

[9] Juhlin L E. Power flow control in a meshed HVDC power transmission network[P].US 20120033462Al,2011.

[10] Barker C D,Whitehouse R S.A current flow controller for use in HVDC grids[C]//10th IET International Conference on AC and DC Power Transmission(ACDC 2012).Birmingham,UK:IET，2012:1-5.

[11] XU Feng, XU Zheng, LIU Gaoren. A Neotype of DC Power Flow Controller and Its Applications in Meshed DC Grids[J].Power System Technology,2014,38(10).

[12] Tianqi Zhang,Chuanyue Li,Jun Liang.A Thyristor Based Series Power Flow Control Device for Multi-Terminal HVDC Transmission.[C]//Power Engineering Conference (UPEC),2014 49th International Universities,IEEE,2014,1-6.

[13] M. P. Bahrman and B. K. Johnson, "The ABCs of HVDC transmission technologies," IEEE Power and Energy Magazine, vol. 5, no. 2, pp. 32-44, 2007.

[14] T. M. Haileselassie and K. Uhlen, "Power system security in a meshed North Sea HVDC grid," Proceedings of the IEEE, vol. lOl, no. 4, pp. 978-990, 2013.

[15] P. Wang, X. P. Zhang, P. F. Coventry, and Z. Li, "Control and protection strategy for MMC MTDC system under converter-side AC fault during converter blocking failure," Journal of Modern Power Systems and Clean Energy, vol. 2, no. 3, pp. 272-281, 2014.

[16] M. Saeedifard and R. Iravani, "Dynamic performance of a modular multilevel back-to-back HVDC system," IEEE Transactions on Power Delivery, vol. 25, no. 4, pp. 2903-2912, 2010.

[17] Q. Mu, J. Liang, Y. Li, and X. Zhou, "Power flow control devices in DC grids," in IEEE Power and Energy Society General Meeting, 2012, pp. 1-7.

[19] L. E. Juhlin, "Power flow control in a meshed HYDC power transmission network," Sep. 30, 2014, US Patent 8,847,430.

[20] A. Lesnicar and R. Marquardt, "An innovative modular multilevel converter topology suitable for a wide power range," in IEEE Power Tech Conference P roceedings, vol. 3, 2003, pp. 1-6.

[21] H. Saad, J. Peralta, S. Dennetiere, J. Mahseredjian, J. Jatskevich, J. Martinez, A. Davoudi, M. Saeedifard, V. Sood, X. Wang et aI., "Dynamic averaged and simplified models for MMC-based HVDC transmission systems," IEEE Transactions on Power Delivery, vol. 28, no. 3, pp. 1723-1730, 2013.

[22] Na Deng, Puyu Wang, Xiao-Ping Zhang, CSEE, Guangfu Tang, and Junzheng Cao"A DC Current Flow Controller for Meshed Modular Multilevel Converter Multi-terminal HVDC Grids," csee journal of power and energy systems, vol. i, no. i, march 2015.

APPENDIX (A)

PARAMETERS OF THE 3-T MESHED MMC-HVDC SYSTEM

Parameter	Value
Nominal AC source Voltage	138 KV (L-N)
Nominal DC Voltage	$\pm$ 50 KV
L_{AC}	150 mH
MMCs rate Capacity	150 MVA
L_{arm}	3 mH
Transformer Voltage Ratio	138 KV/30 KV (Y/Δ)
Nominal AC frequency	50 Hz
Transformer rating	150 MVA
Sub-module capacitor	2,500 μF
Transformer leakage inductance	5%
Branch 12 cable resistance R_{12}	1Ω
R	0.03Ω
Branch 13 cable resistance R_{13}	2Ω
L	1 mH
Branch 23 cable resistance R_{23}	1Ω